

**TIME-DEPENDENT BOND STRENGTH OF CEMENT
SEALING IN ROCK SALT**



**A Thesis Submitted in Partial Fulfillment of the Requirements for the
Degree of Master of Engineering in Geotechnology
Suranaree University of Technology
Academic Year 2014**

กำลังยึดติดของการอุตสาหกรรมในเกลือหินที่ขึ้นกับเวลา



นายชากรีน ปัตตานี

วิทยานิพนธ์นี้เป็นส่วนหนึ่งของการศึกษาตามหลักสูตรปริญญาวิศวกรรมศาสตรมหาบัณฑิต

สาขาวิชาเทคโนโลยีธรณี

มหาวิทยาลัยเทคโนโลยีสุรนารี

ปีการศึกษา 2557

TIME-DEPENDENT BOND STRENGTH OF CEMENT SEALING IN ROCK SALT

Suranaree University of Technology has approved this thesis submitted in partial fulfillment of the requirements for a Master's Degree.

Thesis Examining Committee

(Prof. Dr. Kittitep Fuenkajorn)

Chairperson

(Dr. Prachya Tepnarong)

Member (Thesis Advisor)

(Dr. Decho Phueakphum)

Member

(Prof. Dr. Sukit Limpijumnong)

Vice Rector for Academic Affairs
and Innovation

(Assoc. Prof. Flt. Lt. Dr. Kontorn Chamniprasart)

Dean of Institute of Engineering

ชาگیرิน ปัดตานี : กำลังยึดติดของการอุดซีเมนต์ในเกลือหินที่ขึ้นกับเวลา (TIME-DEPENDENT BOND STRENGTH OF CEMENT SEALING IN ROCK SALT)

อาจารย์ที่ปรึกษา : อาจารย์ ดร.ปรัชญา เทพณรงค์, 85 หน้า.

วัตถุประสงค์ของการศึกษานี้คือ เพื่อทดสอบประสิทธิภาพเชิงกลศาสตร์และพลศาสตร์ของปูนซีเมนต์เพื่อนำมาใช้อุดในชั้นเกลือหินในฟังก์ชันของเวลา ผลการทดสอบที่ได้สามารถช่วยในการออกแบบของซีเมนต์สำหรับการอุดรอยแตกในระยะยาวเพื่อให้มีผลกระทบจากการรั่วไหลในชั้นเกลือหินของเหมืองเกลือให้น้อยที่สุด ผลการทดสอบคุณสมบัติพื้นฐานของซีเมนต์ระบุว่าเมื่อเพิ่มระยะเวลาการบ่มตัว ค่าแรงกดสูงสุดในแกนเดียว ค่าสัมประสิทธิ์ความยืดหยุ่น และค่าแรงดึงแบบบราซิลเลียนของปูนซีเมนต์มีแนวโน้มสูงขึ้น ผลการทดสอบความซึมผ่านของซีเมนต์พบว่าเมื่อระยะเวลาการบ่มตัวเพิ่มขึ้น ค่าความซึมผ่านและค่าสัมประสิทธิ์การซึมผ่านจะลดลง ผลการทดสอบแรงเฉือน โดยตรงระยะสั้นพบว่าแรงเสียดทานยึดติดระหว่างซีเมนต์และเกลือหินมีค่าเท่ากับ 44 องศา และแรงยึดติดมีค่าเท่ากับ 2.12 เมกกะปาสกาล

การทดสอบ Push-out ระยะยาวถูกดำเนินการในแท่งซีเมนต์กับชุดความสัมพันธการบ่มตัวระยะยาวที่ความเค้นเฉือนคงที่ บนพื้นฐานพฤติกรรมการเคลื่อนไหลของความหนืดเชิงยืดหยุ่นเฉือน ความสัมพันธ์ระหว่างการเคลื่อนตัวแนวเฉือนและเวลา โดยระดับความเค้นเฉือนคงที่ต่างๆที่ 30 วัน รูปแบบ Hookean-Kelvin ถูกเลือกเพื่อหาค่าพฤติกรรมการเคลื่อนไหลของความหนืดเชิงยืดหยุ่นเฉือน พารามิเตอร์ที่เหมาะสมของความยืดหยุ่นเฉือน (G_1) ความหนืดเชิงยืดหยุ่นเฉือน (G_2) และสัมประสิทธิ์ความหนืด (η_1) พิจารณาในฟังก์ชันของอัตราส่วนเฉือนคงที่ (τ/τ_{av}) ของแท่งซีเมนต์ในหลุมเจาะ พารามิเตอร์ของ G_1 เพิ่มขึ้นเล็กน้อยเมื่อ (τ/τ_{av}) เพิ่มขึ้น พารามิเตอร์ของ G_2 และ η_1 มีแนวโน้มลดลงเมื่อเพิ่มอัตราส่วนเฉือนคงที่กับความสัมพันธ์เชิงกำลัง การทดสอบแรงเฉือนโดยตรงระยะยาวแสดงรูปแบบพารามิเตอร์การเคลื่อนไหลเฉือน พารามิเตอร์ที่เหมาะสมของ G_1 , G_2 และ η_1 เปลี่ยนแปลงเมื่อเพิ่มอัตราส่วนความเค้นเฉือน (τ/τ_p) ผลการคาดการณ์เป็นไปตามข้อมูลจากการทดสอบเป็นอย่างดี ซึ่งแสดงให้เห็นว่าเป็นรูปแบบการเคลื่อนไหลของความหนืดเชิงยืดหยุ่นแบบไม่เป็นเส้นตรง

สาขาวิชา เทคโนโลยีธรณี

ปีการศึกษา 2557

ลายมือชื่อนักศึกษา _____

ลายมือชื่ออาจารย์ที่ปรึกษา _____

SAKEEREEN PATTANI : TIME-DEPENDENT BOND STRENGTH OF
CEMENT SEALING IN ROCK SALT. THESIS ADVISOR : PRACHYA
TEPNARONG, Ph.D., 85 PP.

SEALING/PUSH-OUT TEST/DIRECT SHEAR TEST/PERMEABILITY

The objectives of this study are to determine the mechanical and hydraulic performance of cement sealing in rock salt as a function of times. The results are used to assist in a long-term design of the cement seals in fracture and dissolved channels to minimize a brine circulation and potential leakage along a main access of a salt mine. The basic mechanical properties test results indicate that when the curing time increases the uniaxial compressive strength, elastic modulus and Brazilian tensile strength of cement grout increases. The results of constant head flow test indicate that when the curing time increases the coefficient of permeability (K) and the intrinsic permeability (k) of cement grout decreases. The short-term direct shear tests results indicate the frictional resistance at cement-salt interface with the friction angle of 44 degrees and cohesion of 2.12 MPa.

The long-term push-out tests are performed on cement plugs with a series of relatively long curing time with the constant shear stress. Base on the visco-elastic shear creep behavior results, the relation between shear displacement and time are obtained with a various constant shear stress levels with 30 days. The Hookean-Kelvin model is chosen to determine the visco-elastic shear creep behavior. The fitting parameters of elastic shear modulus (G_1), visco-elastic shear modulus (G_2) and viscous coefficient (η_1) are determined as function of the applied constant shear ratio (τ/τ_{av}) of borehole cement plug. The empirical parameters, G_1 increase slightly with

the τ/τ_{av} increase. The parameters of G_2 and η_1 tend to decrease in term of increasing applied constant shear ratio with a power relation. The long-term direct shear test results show the shear creep model parameters. The fitting empirical parameters of G_1 , G_2 and η_1 change with the increase in the shear stress ratio (τ/τ_p). The predicted curve agree well with the experiment data, which shows the reasonability of nonlinear visco-elastic shear creep model.



School of Geotechnology

Academic Year 2014

Student's Signature _____

Advisor's Signature _____

ACKNOWLEDGMENTS

I wish to acknowledge the funding supported by Suranaree University of Technology (SUT).

I would like to express my sincere thanks to Dr. Prachya Tepnarong for his valuable guidance and efficient supervision. I appreciate his strong support, encouragement, suggestions and comments during the research period. My heartiness thanks to Prof. Dr. Kittitep Fuenkajorn and Dr. Decho Phueakphum for their constructive advice, valuable suggestions and comments on my research works as thesis committee members. Grateful thanks are given to all staffs of Geomechanics Research Unit, Institute of Engineering who supported my work.

Finally, I would like to thank beloved parents for their love, support and encouragement.

Sakeereen Pattani

TABLE OF CONTENTS

	Page
ABSTRACT (THAI)	I
ABSTRACT (ENGLISH)	II
ACKNOWLEDGEMENTS	IV
TABLE OF CONTENTS	V
LIST OF TABLES	VIII
LIST OF FIGURES	XI
SYMBOLS AND ABBREVIATIONS	XIV
CHAPTER	
I INTRODUCTION	1
1.1 Background and rationale	1
1.2 Research objectives	1
1.3 Research methodology	2
1.3.1 Literature review	3
1.3.2 Sample preparation	3
1.3.3 Laboratory testing	4
1.3.4 Calibration of creep parameters	5
1.3.5 Discussions and conclusions	6
1.3.6 Thesis writing and presentation	6
1.4 Scope and limitations	6
1.5 Thesis contents	7

TABLE OF CONTENTS (Continued)

	Page
II LITERATURE REVIEW	8
2.1 Rock Salt in Northeast Region of Thailand	8
2.2 Mechanical Properties of Rock Salt.....	9
2.3 Borehole Sealing in Rock Salt	12
2.4 Bond Strength of Cement Grout	14
2.5 Direct Shear Creep Test	24
2.6 Permeability Properties of Rock Salt and Cement Grout	26
III CEMENT GROUT AND ROCK SALT SPECIMENTS	
PREPARATION	28
3.1 Cement Grout Preparation	28
3.1.1 Apparatus	28
3.1.2 Procedure for preparing cement borehole plugs	29
3.2 Rock Salt Specimen	37
IV LABORATORY TESTING.....	41
4.1 Introduction.....	41
4.2 Basic Mechanical Properties Tests of Cement Grout	41
4.2.1 Viscosity and slurry density of cement grout	41
4.2.2 Uniaxial compressive strength tests.....	43
4.2.3 Brazilian tensile strength tests	43
4.3 Push-out test.....	51
4.4 Direct shear test.....	57

TABLE OF CONTENTS (Continued)

	Page
4.5 Permeability tests of cement grout.....	61
V CALIBRATION OF CREEP PARAMETERS	65
5.1 Objective.....	65
5.2 Visco-elastic shear creep model	65
5.3 Creep parameters of push-out tests.....	67
5.4 Creep parameters of long-term direct shear tests	70
VI DISCUSSIONS, CONCLUSIONS AND	
RECOMMENDATIONS FOR FUTURE STUDIES	73
6.1 Discussions and conclusions.....	73
6.2 Recommendations for future studies	76
REFERENCES	77
BIOGRAPHY	85

LIST OF TABLES

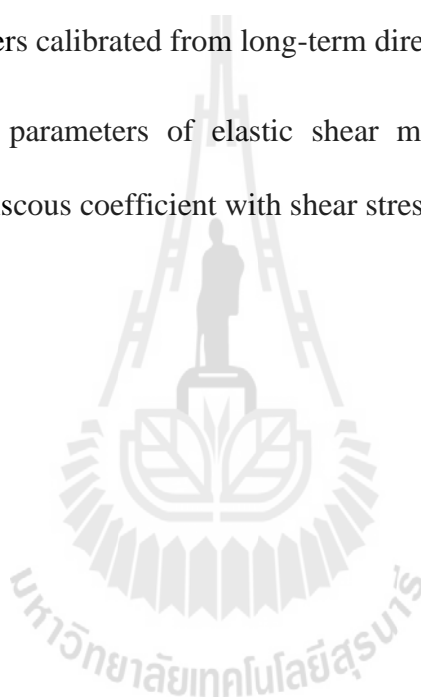
Table	Page
2.1 Component of BCT-1F and BCT-1FF grouts (Gulick et al., 1980, as quoted by Roy et al., 1985).....	19
2.2 Mixture Proportions of Five Four-Year-Old Grouts (Boa, 1978, as quoted by Roy et al., 1985).....	20
2.3 Mixture 80-081 (PSU/WES) Proportions (Roy et al., 1982, as quoted by Roy et al., 1985).....	20
2.4 Composition of Mixtures 83-03, 83-05 and 83-06 (Wakeley and Roy,1985).....	21
2.5 Compositions of Formulations 82-030, 82-14 and 82-02 (Roy et al., 1983, as quoted by Roy et al., 1985).....	22
3.1 Weight composition of Salt-bond II cement (SBII and SBIII).....	31
3.2 Specimen dimensions prepared for uniaxial compressive strength testing and elastic modulus measurement.....	31
3.3 Specimen dimensions prepared for Brazilian tensile strength testing.....	33
3.4 Cement grout specimen prepared for long-term permeability testing.....	35
3.5 Depth and specimen dimensions of rock salt and cement plugs prepared for push-out testing.....	38
3.6 Depth and specimen dimensions of rock salt prepared for direct shear testing.....	38

LIST OF TABLES (Continued)

Table	Page
4.1 Viscosity and slurry density of cement slurry.....	42
4.2 Uniaxial compressive strength (σ_c) and elastic modulus (E) of Salt-bond II cement with a low brine content (SBII).....	46
4.3 Uniaxial compressive strength (σ_c) and elastic modulus (E) of Salt-bond II cement with a high brine content (SBIIH).....	47
4.4 Summary of the Brazilian tensile strength tests (σ_B) of Salt-bond II cement with a low brine content (SBII).....	48
4.5 Summary of the Brazilian tensile strength tests (σ_B) of Salt-bond II cement with a high brine content (SBIIH).....	49
4.6 Summary of the uniaxial compressive strength (σ_c) tests, elastic modulus (E) measurements and Brazilian tensile strength tests (σ_B) of cement plugs...	50
4.7 Summary of the push-out tests.....	56
4.8 Summary of shear strength parameters calibrated from direct shear tests using Coulomb's criteria.....	58
4.9 Constant normal stress and constant shear stress for long-term direct shear tests.....	60
4.10 Summary of permeability testing of grouting.....	64
5.1 Creep parameters calibrated from push-out test results.....	68

LIST OF TABLES (Continued)

Table		Page
5.2	The empirical parameters of elastic shear modulus, visco-elastic shear modulus and viscous coefficient with bond stress ratio.....	69
5.3	Creep parameters calibrated from long-term direct shear test results.....	71
5.4	The empirical parameters of elastic shear modulus, visco-elastic shear modulus and viscous coefficient with shear stress ratio.....	72



LIST OF FIGURES

Figure	Page
1.1 Research Methodology.....	2
2.1 Map of Southeast Asia showing locations of the Khorat and the Sakon Nakon salt basins on the Khorat Plateau, northeastern Thailand (Tabakhet al., 2002).....	9
2.2 The typical deformation as a function of time of creep materials (modified after Jeremic, 1994).....	11
3.1 Bag of Portland-pozzolan cement 50 kg is used in this study.....	30
3.2 PVC molds with curing cement mixture.....	35
3.3 Some of specimens prepared for mechanical characterization testing.....	36
3.4 Cement grout cylinders within the PVC mold for permeability testing.....	36
3.5 Push-out test specimens is drilled with 25 mm diameter holes perpendicular to the bottom.....	39
3.6 Some of rock salt specimens prepared for the push-out testing.....	39
3.7 Salt core is dry-cut by a cutting machine.....	40
3.8 Saw cut surfaces and cement-rock salt interface are prepared for the direct shear testing.....	40
4.1 Brookfield® viscometer model RV (ASTM D2196).....	42
4.2 Uniaxial compressive strength tests.....	44
4.3 Uniaxial compressive strengths (σ_c) as a function of curing time.....	44

LIST OF FIGURES (Continued)

Figure	Page
4.4	Brazilian tensile strength tests.....45
4.5	Brazilian tensile strengths (σ_B) as a function of curing time.....45
4.6	Schematic drawing of the push-out test setup, 1.Loading frame; 2.Hydraulic cylinder; 3.Steel plate with a slit; 4.Square steel plate; 5.Axial bar and steel cylinder; 6.Square steel plate frame; 7.Rock salt sample; 8.Cement grout plug; 9.PVC mold; 10., 11. and 12.Dial gages.....53
4.7	The push-out test setup.....53
4.8	Applied shear stress as a function of the top and the bottom axial cement plug displacements for push-out tests.....54
4.9	A cut section of specimen no. SBIIH-04-07-PO-01 after failure in the push- out test.....55
4.10	Top plug displacement (δ_T) as a function of time for push-out tests.....55
4.11	The direct shear machine model EL-77-1030 for direct shear tests.....57
4.12	Shear stress as a function of shear displacement for SBIIH specimens.....58
4.13	Shear stress as a function of normal stress for SBIIH specimens.....58
4.14	The direct shear machine model DR-44 for long-term direct shear tests.....59
4.15	Shear displacements (δ_s) as a function of time for long-term direct shear tests with a constant normal stress of 1.86 MPa.....60
4.16	Constant head flow test apparatus used for the permeability testing of a cement grout.....62

LIST OF FIGURES (Continued)

Figure	Page
4.17 Coefficient of permeability (K) of the cement grouts.....	63
4.18 Intrinsic permeability (k) of the cement grouts.....	63
5.1 Hookean-Kelvin model (Yang and Cheng, 2011).....	66
5.2 The push-out test results (points) and back predictions (lines).....	67
5.3 Influence of applied stress ratio (τ/τ_{av}) on the elastic shear modulus (G_1), visco-elastic shear modulus (G_2) and viscous coefficient (η_1).....	69
5.4 The long-term direct shear test results (points) and back predictions (lines)...	71
5.5 Influence of shear stress ratio (τ/τ_p) on the elastic shear modulus (G_1), visco-elastic shear modulus (G_2) and viscous coefficient (η_1).....	72



SYMBOLS AND ABBREVIATIONS

σ_c	=	Uniaxial compressive strengths
σ_B	=	Brazilian tensile strengths
E	=	Elastic modulus
σ_1	=	Major principal stress
σ_2	=	Intermediate principal stress
σ_3	=	Minor principal stress
σ_m	=	Mean stress
τ_{oct}	=	Octahedral shear stress
ϵ_e	=	Instantaneous elastic strain
ϵ_p	=	Permanent strain
σ_n	=	Constant normal stress
c_p	=	Cohesion
τ_p	=	Peak shear strength
τ_r	=	Residual shear strength
ϕ_p	=	Peak friction angles
ϕ_r	=	Residual friction angles
τ	=	Constant shear stress
τ_{av}	=	Bond strength or Average shear stress
F	=	Failure load

SYMBOLS AND ABBREVIATIONS (Continued)

D_i	=	Plug diameter
L_c	=	Plug length
k_n	=	Normal stiffness
k_s	=	Shear stiffness
K	=	Coefficient of permeability
k	=	Intrinsic permeability
Q	=	Volume flow rate
A	=	Cross-sectional area of cement grout
i	=	Hydraulic gradient
μ	=	Dynamic viscosity of brine
γ	=	Density of brine
δ	=	Shear displacements
δ_0	=	Instantaneous shear displacement
t	=	Time
G_1	=	Elastic shear modulus
G_2	=	Visco-elastic shear modulus
η_1	=	Viscous coefficient
δ_T	=	Top plug displacements of push-out tests
δ_s	=	Shear displacements of direct shear tests
τ/τ_{av}	=	Applied constant shear ratio
τ/τ_p	=	Shear stress ratio

SYMBOLS AND ABBREVIATIONS (Continued)

χ	=	Empirical parameters
κ	=	Empirical parameters
α	=	Empirical parameters
β	=	Empirical parameters
λ	=	Empirical parameters
ω	=	Empirical parameters



CHAPTER I

INTRODUCTION

1.1 Background and rationale

Design of seals is required in sealing mine openings in order to control mine effluents. Generally, cementing materials are used to seal fractures and dissolved channels to prevent brine leakage along the openings. The primary function of borehole and shaft seals is to reduce hydraulic conductivity of the openings to an acceptable level. Axial load on plugs or seals in an underground salt mine leads to shear stresses along a contact between the plug and a host rock. These shear stresses may cause cracking and increase permeability along the cement plug and rock interfaces. Under extreme condition they can cause slipping of the cement plugs. Therefore, a bond between plug and rock is a critical element of the design and performance of plug in the excavated openings (Fuenkajorn and Daemen, 1996; Akgun and Daemen, 1997; Tepnarong, 2012).

1.2 Research objectives

The objectives of this study are to determine the bond strength of cement grout borehole plugs cast in rock salt cylinders through the push-out testing, and to determine the shear strength between cement-salt interfaces by the direct shear testing as a function of cement curing period. The results are used to assist in a long-term design of the cement seals in fracture and dissolved channels to minimize a brine

circulation and potential leakage along a main access of salt mines in the northeastern area of Thailand.

1.3 Research methodology

The research methodology shown in Figure 1.1 comprises six steps; literature review, sample preparation, laboratory testing, calibration of creep parameters, discussions and conclusions, and thesis writing.

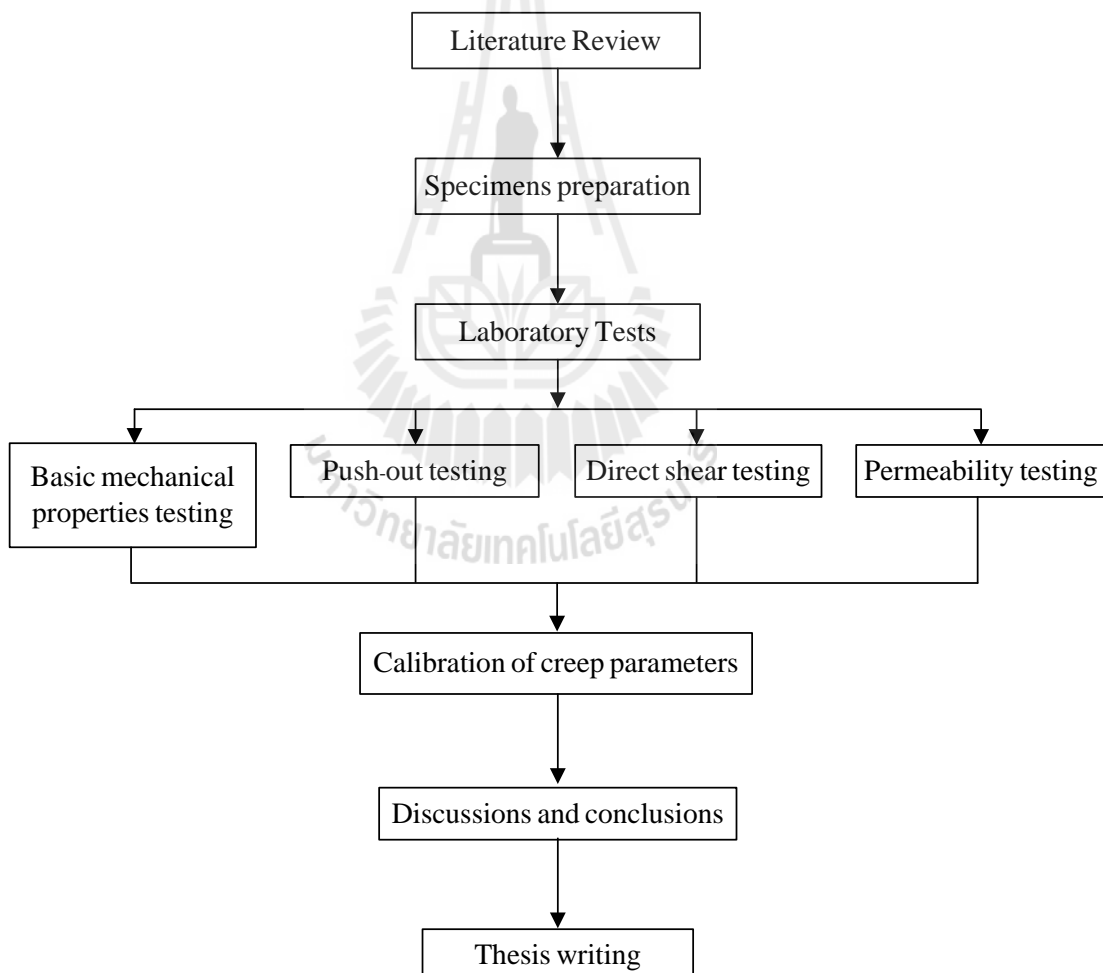


Figure 1.1 Research Methodology

1.3.1 Literature review

Literature review were carried out by studying the previous researches of time-dependent bond strength between cement grouts and rock salt. The sources of information are from text books, journals, technical reports and conference papers. A summary of the literature review is given in chapter two.

1.3.2 Specimens preparation

1.3.2.1 Cement grout preparation

The cement mixing for the borehole plugs and the direct shear testing specimens was prepared according to the API No. 10 (American Petroleum Institute, 1986; Akgun and Daemen, 1997) by mixing the cement with a salt (NaCl) saturated brine. The constituents of cement slurry were commercial grade Portland cement mixed with chloride resistant agent, NaCl saturated brine, anti-form agent and a liquid additive including expansion. The brine was prepared by dissolving clean rock salt in distilled water. Portland-pozzolan cement was chosen due to its low brine demand, sulfate resistance and widely used in construction industry. A liquid additive contributed to expansiveness of mixture. An anti-forming agent was used to decrease the air content of the cement slurry and to ease a control of cement slurry weight and volume.

1.3.2.2 Rock salt specimens

100 mm diameter core samples of rock salt are donated by Asian Potash Mining Company. They were collected from a borehole located in Bumnetnarong district, Chaiyaphum province. All samples are obtained from the Middle Salt Member at depths between 70 m and 130 m of the Maha Sarakham formation. Sample preparations were followed the ASTM D4543 standard practice,

as much as practical. Specimens were prepared for the direct shear strength tests and the push-out tests with length of 100 mm. The cylindrical push-out specimens were drilled with 25 mm diameter holes perpendicular to the bottom sample surfaces. The saw cut surfaces were prepared for the direct shear testing.

1.3.3 Laboratory testing

1.3.3.1 Basic mechanical properties tests of cement grout

The basic mechanical properties test include viscosity and slurry density of cement grout, uniaxial compressive strength (σ_c), elastic modulus (E) and Brazilian tensile strength (σ_B). Specimens of 54 mm diameter cylindrical cement specimens with length to diameter ratios between 2.5 and 3.0 were prepared by curing cement pastes in PVC molds for 1, 3, 7, 14, 21 and 28 days. They were cured at room temperature (ASTM C192). Each mold was puddled with the puddling rod to eliminate cement segregation. The remaining portion of the molds was filled with brine. All cement cylinders were taken out of their molds after each curing period. The ends of specimen were cut and paralleled.

Viscosity measurement followed, as much as practical, ASTM D2196. The viscosity is measured with Brookfield® viscometer.

The uniaxial compressive strength test procedure was followed, as much as practical, the ASTM standards (D7012 and C39). The cement grouts were loaded at the constant rate of 0.1-0.5 MPa/s until failure. The axial displacements were monitored by displacement dial gauges

The Brazilian tensile strength tests were performed in accordance with ASTM standard (D3967). The load was applied along the diameter of the specimen until failure occurred.

1.3.3.2 Push-out tests

The objective of this test is to determine the axial mechanical strength and long-term deformation of borehole plugs in the rock salt core through the push-out tests. The curing period for push-out tests was 7 days.

1.3.3.3 Direct shear tests

The shearing resistance between cement grout and rock salt fracture is determined by the direct shear testing. The test procedure is similar to the ASTM D5607 standard practice. The cement slurry was casted on 100 mm diameter saw cut fracture surfaces. The cement was cured for 7 days prior to testing for all tests.

1.3.3.4 Permeability tests of cement grout

The permeability of the grouting materials is determined in term of the intrinsic permeability (k). The constant head flow test was conducted to measure the longitudinal permeability of the grout. The cylinder specimen was 100 mm in diameter and 100 mm long. After three days of curing, the specimen was carefully removed from the cast (PVC pipe), cleaned, and placed in a brine bath before installing in the permeability test apparatus. The permeability of the test system was measured and recorded at 1, 3, 7, 14, 21, 28, 35, 42, 60, 109, 136 and 254 days of curing periods.

1.3.4 Calibration of creep parameters

The test results were used to determine the displacement and transient creep parameters. The regression analysis of the proposed shear creep strain equation with the IBM SPSS Statistics 19 (Wendai, 2000) is performed to determine the elastic shear modulus, the visco-elastic shear modulus and visco-coefficient.

1.3.5 Discussions and conclusions

Discussions of the results are described to determine the reliability and accuracy of the measurements. The results can reveal the relationship can be used to between the bond strength of cement sealing and the curing periods, and develop the mathematical relations for time-dependent bond strength prediction.

1.3.6 Thesis writing and presentation

All research activities, methods, and results are documented and compiled in the thesis. The research or findings is published in the conference proceedings.

1.4 Scope and limitations

The scope and limitations of the research include;

1. All tests were conducted on rock salt specimens obtained from the Middle Salt member of the Maha Sarakham formation in northeastern Thailand.
2. The cement grout was prepared from the commercial grade Portland-pozzolan cement mixed with chloride resistant agent and NaCl saturated brine.
3. The push-out test was performed with the 100 mm diameter core, with length of 100 mm, and the 25 mm diameter hole for cement grout plugs.
4. The direct shear test was performed 100 mm diameter core of rock salt and cement cast.
5. The time-dependent tests including push-out test and long-term direct

shear test were conducted up to 30 days of constant loading rate or until failure.

6. All tests were conducted under ambient temperature.

1.5 Thesis contents

Chapter I describes the objectives, the problems and rationale, and the methodology of the research. **Chapter II** summarizes results of the literature review. **Chapter III** describes the sample preparation. **Chapter IV** describes the laboratory testing and test results. **Chapter V** describes calibration of creep parameters. **Chapter VI** summarizes the research results, and provides recommendations for future research studies.

CHAPTER II

LITERATURE REVIEW

Introduction

The topics reviewed here include rock salt in Thailand, rock salt properties, borehole sealing in rock salt, the bond strength between rock salt and cement grout, the direct shear creep test and permeability properties of rock salt and cement grout.

2.1 Rock Salt in Northeast Region of Thailand

Rock salt formation in Thailand is located on the Khorat plateau as shown in Figure 2.1. The Khorat plateau covers 150,000 square kilometers, from 14° to 19° northern latitude and 101° to 106° eastern longitude. The northern and eastern edges of the plateau lie close to Laos and the southern one close to Cambodia (Utha-aroon, 1993).

Rock salt is separated into 2 basins: Sakon Nakhon Basin and Khorat Basin. The Sakon Nakhon Basin in the north is about 17,000 square kilometers. It covers the area of Nong Khai, Udon Thani, Sakon Nakhon, Nakhon Phanom, and Mukdahan provinces and extends to some part of Laos. The Khorat Basin is in the south, which has about 33,000 square kilometers. The basin covers the area of Nakhon Ratchasima, Chaiyaphum, Khon Kaen, Maha Sarakham, Roi Et, Kalasin, Yasothon, Ubon Ratchathani provinces and the north of Buriram, Surin and Sisaket provinces (Suwanich, 1986).

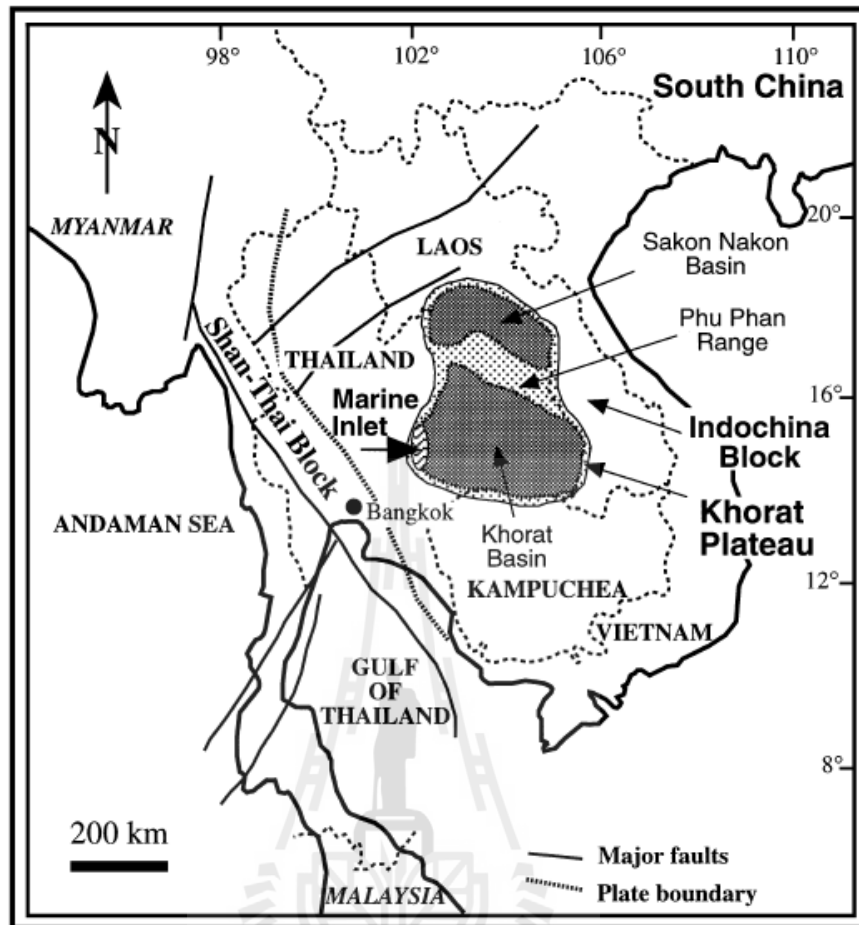


Figure 2.1 Map of Southeast Asia showing locations of the Khorat and the Sakon Nakhon salt basins on the Khorat Plateau, northeastern Thailand (Tabakh et al., 2002).

2.2 Mechanical Properties of Rock Salt

The time-dependent deformation (or creep) is the process at which the rock can persist deformation without changing stress. The creep strain seldom recovers fully when loads are removed, thus it is largely plastic deformation. Creep deformation occurs in three different phase, as shown in Figure 2.2, which relatively represent a model of salt properties undergoing creep deformation due to the sustained constant load. Upon application of a constant force on the rock salt, an

instantaneous elastic strain (ϵ_e) is induced. The elastic strain is followed by a primary or transient strain, shown as Region I. Region II, characterized by an almost constant slope in the diagram, corresponds to secondary or steady state creep. Tertiary or accelerating creep leading to rather sudden failure is shown in Region III. Laboratory investigations show that removal of applied load in Region I at point L will cause the strain to fall rapidly to the M level and then asymptotically back to zero at N. The distance LM is equal to the instantaneous strain ϵ_e . No permanent strain is induced here. If the removal of stress takes place in the steady-state phase the permanent strain (ϵ_p) will occur. From the stability point of view, salt structure deformations after constant load removal have only academic significance, since the stresses imposed underground due to mining operations are irreversible. The behavior of the salts with time-dependent deformation under constant load is characterized as a visco-elastic and visco-plastic phenomenon. Under these conditions the strain criteria are superior to the strength criteria for design purposes, because failure of most salt pillars occurs during accelerated or tertiary phase of creep, due to the almost constant applied load. The dimensions of a pillar in visco-elastic and visco-plastic rock should be established on the basis of a prediction of its long-term strain, to guard against adequate safety factor accelerating creep (Fuenkajorn and Daemen, 1988; Dusseault and Fordham, 1993; Jeremic, 1994; Knowles et al., 1998).

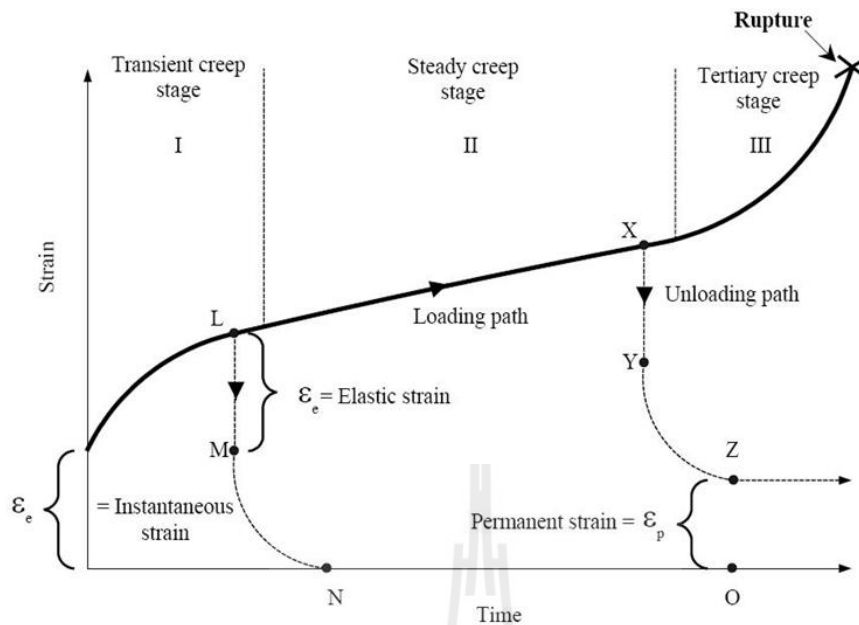


Figure 2.2 The typical deformation as a function of time of creep materials (modified after Jeremic, 1994).

Samsri et al. (2010) determined the effect of the intermediate principal stress on the time-dependent behavior of rock salt obtained from the Maha Sarakham formation. A polyaxial creep frame applied constant principal stresses to cubical shaped specimens with a nominal dimension of $5.4 \times 5.4 \times 5.4 \text{ cm}^3$. The applied octahedral shear stresses (τ_{oct}) varied from 5, 8, 11 to 14 MPa while the mean stress (σ_m) was maintained constant at 15 MPa for all specimens. The loading conditions ranged from the triaxial ($\sigma_1 \neq \sigma_2 = \sigma_3$) to the polyaxial ($\sigma_1 \neq \sigma_2 \neq \sigma_3$ and $\sigma_1 = \sigma_2 \neq \sigma_3$) stress states. The Burgers model was used to describe the elastic, visco-elastic (transient) and visco-plastic (steady-state) behavior of the salt. The specimen deformations were monitored along the three principal axes for up to 21 days. Regression analyses on the octahedral shear strain-time curves suggested that the salt elastic modulus tended to be independent of the intermediate principal stress (σ_2). It however tended to

increase as the applied τ_{oct} increases. Under the same magnitude of τ_{oct} the visco-elastic and visco-plastic parameters increased when σ_2 increased from the triaxial condition, $\sigma_2=\sigma_3$, to the condition where $\sigma_2=\sigma_1$.

Fuenkajorn and Phueakphum (2010) performed cyclic loading tests on the Maha Sarakham salt. Their results indicated that the salt compressive strength decreased with increasing number of loading cycles, which could be best represented by a power equation. The salt elastic modulus decreased slightly during the first few cycles, and tends to remain constant until failure. It seemed to be independent on the maximum loads. Axial strain–time curves compiled from loci of the maximum load of each cycle apparently showed a time-dependent behavior similar to that of creep tests under static loading. In the steady-state creep phase, the visco-plastic coefficients calculated from the cyclic loading test were about an order of magnitude lower than those under static loading. The salt visco-plasticity also decreased with increasing loading frequency. Surface subsidence and cavern closure simulated using parameters calibrated from cyclic loading test results were about 40% greater than those from the static loading results. This suggested that application of the property parameters obtained from the conventional static loading creep test to assess the long-term stability of storage caverns in salt with internal pressure fluctuation might not be conservative.

2.3 Borehole Sealing in Rock Salt

Types of borehole sealing have been classified by various industries, based on their sealing objectives. For example, Gray and Gray (1992) classified the sealing of mine openings and boreholes into three categories: permanent, temporary, and semi-

permanent sealing. Smith (1994) classified the sealing of groundwater wells into three categories: temporary sealing, sealing actively used boreholes, and sealing for permanent decommissioning. Daemen and Fuenkajorn (1996) classified borehole sealing into two main categories: (1) sealing actively used boreholes and (2) sealing unused boreholes.

Sealing actively used boreholes involved sealing of the annular zone between casing or pipe and the host rock and sealing of open boreholes that would be used in the future. The reasons for sealing of actively used boreholes were to protect the casing from corrosion, to prevent blowouts by quickly forming a seal, to protect the casing from shock loads in drilling deeper, and to seal off zones of circulation or thief zones (Economides et al, 1998).

Sealing unused boreholes represents permanent sealing, which mainly involved sealing of any abandoned boreholes or wells. The primary function of seals for unused boreholes was to isolate zones of gas or liquid, which mainly emphasizes on environmental protection (Daemen and Fuenkajorn, 1996). The reasons for sealing of unused boreholes were to prevent groundwater contamination, to prevent poor aquifer groundwater from moving between water-bearing zones, to conserve aquifer yield and artesian pressure, and to remove any physical hazard (Smith, 1993).

Fuenkajorn and Daemen (1987) studied mechanical relationship between cement, bentonite and surrounding rock. The study dealt with the mechanical interaction between multiple plugs and surrounding rock and identification of potential failure. Two conceptual plug designs were studied. Pipe tests were performed to determine the swelling pressures of 60 mm diameter bentonite plugs and of 64 mm diameter cement plugs. The axial and radial swelling pressures of a

bentonite plug specimen were 7.5 and 2.6 MPa after adsorbing water for 5 days. The maximum radial expansive stresses of the cement plugs cured for 25 days were 4.7 and 2.7 MPa for system 1 and system 3 cement. Results from the experiment indicated that in order to obtain sufficient mechanical stability of bentonite seal, the sealing should be done below groundwater level. If cement material was used to seal in hard rock, the mechanical stability would be higher than sealing in soft rock.

2.4 Bond Strength of Cement Grout

Akgun (1996) conducted a research on bond strength of cement grout seals in rock. The objective of the research was to study the relationship between the strength of cement grout and the length-to-radius ratio of cement specimen. The strength values (axial strength, bond strength, and peak shear strength) were obtained from the push-out tests of the cement grout borehole plugs with various diameter and length placed in welded tuff cylinders. The results from the test showed that the three strength measures decreased with increasing plug radius and with decreasing plug length. The specimen with plug the length-to-radius ratio of eight had the highest axial strength. The result of the test indicated that in order to gain enough mechanical stability in permanently sealing of borehole with cement, length-to-radius ratio of cement grout should equal or greater than eight.

Ouyang and Daemen (1996) carried out the experiments on borehole sealing in rock by using bentonite and mixture of bentonite and crushed tuff. The experiment included laboratory investigation of the sealing performance of bentonite and of bentonite mixed with crushed tuff plugs under various conditions. Permeability tests of the samples included longitudinal flow test, polyaxial permeability test, high-

temperature permeability test, and piping test. The mixture of bentonite and crushed tuff was consisted of 15%, 25% and 35% by weight of bentonite. Results of longitudinal flow test reveal that permeability value was low when high coefficient of uniformity crushed rock was used in the bentonite mix. The permeability decreased as quantity of bentonite increased. Results of polyaxial permeability test showed that the permeability in horizontal flow was higher than that in vertical flow. The differential permeability between the two directions increased as quantity of bentonite increased. Results of high-temperature permeability test indicated that the highest permeability value was at temperature of 35 °C, and at temperature of 60 °C. Results of piping test revealed that permeability in the vertical flow did not change when water was allowed to drain out from the hole provided at the bottom while water flow out from the side hole was less than 2%. Results of testing indicated that by using bentonite mixed with crushed tuff as sealing material, the quantity of bentonite should not be less than 35% by weight. The crushed rock or coarse grain aggregate should be well graded and should have the minimum coefficient of uniformity of 16. The mixing and compaction should meet the standard proctor compaction or higher than the standard.

South and Fuenkajorn (1996) presented an experimental method to assess the performance of cement borehole seals (plugs) under laboratory conditions. The prime goals of the experiment were to obtain experimental data regarding the effectiveness of sealing. The conceptual approach used to evaluate borehole seal in the study was to compare flow through a sealed borehole in rock with flow through intact rock under varying stress conditions. The intact rock specimen was placed under axial and confining stresses to simulate stress field at depths of about 1000,

600, and 300 m. The intact rock was tested, and the rock bridge cored from the specimen. The plug was placed and tested while the specimen remains under the stress field. The results from the test suggested that flow rate through the specimens with the same permeability with those of the cement and surrounding rock. The analysis by computer simulation showed a linear flow rate in specimen that permeability ratio of cement to surrounding rock exceeds 100. The tension zone did not increase when the stress from cement expansion is less than 75 % of tangential stress acting at the borehole wall.

Akgun (1997) conducted a series of push-out tests to determine the suitable material to seal a large borehole in rock salt formation. The adopted material in his study and testing was cement which had two different expansion properties, self-stress I cement and salt-bond II cement. The self-stress I was the mix between 659 g of self-stress cement and 493 g of NaCl-saturated brine. The salt-bond II cement was formed by 1000 g of class H, 450 g of NaCl-saturated brine, 64 g of liquid additive D604 and 4.4 g of anti-foam agent (M45). The rock salt cylinder specimen was hollowed out. Cement was filled in the rock salt specimens with the length to radius ratio of two. The specimens were cured for eight days before testing. Results of testing showed that friction between self-stress cement and rock specimen was 2.2 MPa or 22% of friction between rock salt itself, whereas friction between salt-bond cement and rock specimen was 6.1 MPa or 60% of friction between rock salt itself. In order to obtain sufficient mechanical stability of borehole sealing, salt-bond II cement was recommended.

Ran et al. (1997) studied the dynamic compaction properties of bentonite. The objective of the study was to determine the properties of bentonite seal and to

evaluate the method of dynamic compaction for an effective bentonite shaft seal. Extensive laboratory dynamic compaction tests were conducted to study the densification of granular bentonite mixed with distilled and deionized water or with brine from the Waste Isolation Pilot Plant (WIPP). Results from the test revealed that the dynamic compaction can densify bentonite to a dry density of 1.86 Mg/m^3 when mixed with WIPP brine and 1.74 Mg/m^3 when mixed with distilled and deionized water. At these densities bentonite exhibited permeabilities in the order of 10^{-19} m^2 . Therefore, for using compacted bentonite as a sealing material, saline water was recommended in the mix because it should result in a higher dry density, lower porosity and lower permeability than the distilled water.

Akgun and Daemen (2002) studied the degrees of saturation of the cement plugged cylinder that affected strength of the expansive cement by conducting push-out test. The study factor included the relationship between the degree of saturation versus the strength of cement, as well as the radius of sealing sample versus the strength of cement. Rock specimen was a cylinder shaped tuff with hollowed out at the center. Radius of the hollows were 6.35, 12.70, 25.40 and 50.80 mm. The outer radius ranged between 38.10 and 93.66 mm. Degree of saturation of the test samples were divided into three levels 1) completely dry, 2) low saturated degree, and 3) medium saturated degree. The tests revealed that the axial strength (friction between cement and rock) and the shear strength were high in the sample with higher degree of saturation, and were lower in the smaller specimen diameter. The results from the test indicated that in order to obtain low permeability and high strength seals, the location of cement sealing should be submersed in groundwater.

Akgun and Daemen (2004) studied an expansive cementitious borehole plug emplaced in an underground opening in the vicinity which generated radial stresses on the walls of the opening due to an axial stress applied to the borehole plug due to plug swelling. As these radial stresses might lead to the tensile fracturing of the rock, minimizing or preferably eliminating tensile stresses in rock was particularly important to preserve waste containment. Presents the theoretical radial (normal) stress distribution and tensile strength in a borehole plug-rock system due to combined axial, thermal and lateral loading, along with analysis indicated that the mean tensile strength of rock exceeded the tensile strength of in-situ borehole plugs, and suggested that the rock hosting in-situ borehole plugs was fairly stable against tensile fracturing. The tensile strengths of rock measured in this study represented low bounds due to the absence of confining pressure.

Field studies in the 1970's in Kansas and in New Mexico provided data about the cementitious mixtures designed to be compatible with evaporites, comparisons were made with regard to grout formulations, compressive strength and bond strength. Formulation of the BCT-1F and BCT-1FF grouts (Table 2.1) followed extensive laboratory-based trial mixing and testing by the U.S Army Engineering Waterways Experiment Station (WES), Dowell, The Pennsylvania State University (PSU), and Oak Ridge National Laboratory (ORNL). The compressive strength of the BCT-1F sample ranges from 23.25 to 79.05 MPa and push-out bond strength vary from 2.48 to 7.15 MPa, and compressive strength of the BCT-1FF grouts which ranged from 20.84 to 131.79 MPa and Push-out bond strength ranged from 2.69 to 14.21 MPa.

Table 2.1 Component of BCT-1F and BCT-1FF grouts (Gulick et al., 1980, as quoted by Roy et al., 1985).

Proportions (wt %)	BCT-1F	BCT-1FF
Class H cement	50.10	52.20
Expansive additive	6.70	7.00
Flyash (high lime)	16.90	17.60
Salt (NaCl)	6.50	-
Dispersant	0.20	0.20
Defoamer	0.02	0.02
Water	19.50	23.00

U.S Army Engineering Waterways Experiment Station (WES) studied the Four-year-old Grouts had begun to formulate and test potential cementitious mixtures for the use at the Waste Isolation Pilot Plant (WIPP) site prior to the ERDA-10 experiments. Compositions of five of these grout mixtures were presented in Table 2.2. Reports compressive strengths of samples cured for 28 days at 53 °C ranged from 34.9 to 61.96 MPa. Push-out bond strengths ranged minimum of BP-521-25 MP was 1.73 MPa and maximum of BPN-FA-BS-SP-P-1 (Type III) was 5.97 MPa.

The 80-081 Grout (so-called PSU/WES mixture) was intermediate in composition between the BCT-1F and BCT-1FF formulations. The composition of this mixture is given in Table 2.3. The compressive strength of 80-081 grouts specimens which ranged from 43.2 to 107.7 MPa.

Table 2.2 Mixture Proportions of Five Four-Year-Old Grouts (Boa, 1978, as quoted by Roy et al., 1985).

Material (lb/ft ³)	BP-521-25 MP	BPN-FA-SP-P	BPN-CS-FA-1	BPN-FA-BS-SP-P-1	BPN-FA-BS-SP-P-1 (Type III)
ChemComp cement	43.54	61.12	62.02	55.21	-
ChemStress cement	9.00	-	9.00	-	-
Cement Type III	-	-	-	-	55.21
Fly ash	12.40	20.56	16.76	18.58	18.58
Natural salt	-	-	-	11.43	11.43
TUFA	9.84	-	-	-	-
Melment L-10	2.10	1.63	1.72	1.48	1.48
Plastiment (oz/ft ³)	2.76	2.60	3.02	2.94	2.94
Water	36.14	34.31	32.66	31.73	31.73

Table 2.3 Mixture 80-081 (PSU/WES) Proportions (Roy et al., 1982, as quoted by Roy et al., 1985).

Formulation	Mass (grams)
Class H cement	68.00
Fly ash	22.90
Expansive additive	8.34
NaCl	4.05
Water reducer	1.10 mL
Defoaming agent	0.02
Freshly boiled deionized water	27.40

Mixture 83-03 was a salt-containing mixture related to the BCT-1F formulation, mixtures 83-03 and 83-05 were formulated for use in halite and contain salt, mixture 83-06 was a salt-free formulation to be used in anhydrite. Mixture

compositions are presented in Table 2.4. The compressive strength of the 83-03, 83-05 and 83-06 grouts ranged from 22.07 to 97.00 MPa, 32.30 to 53.10 MPa, and 53.50 to 113.90 MPa, respectively. The push-out bond strength tests on 83-06 varied from 1.02 to 3.33 MPa.

Grout Formulations 82-02, 82-03 and 82-14. The compositions of formulations are given in Table 2.5. The compressive strength of the 82-02, 82-03 and 82-14 grouts ranged from 11.8 to 64.4 MPa, 74.9 to 128.2 MPa, and 28.7 to 60.7 MPa, respectively.

Table 2.4 Composition of Mixtures 83-03, 83-05 and 83-06 (Wakeley and Roy, 1985).

Component	Mixture		
	83-03	83-05	83-06
(wt % of total)			
Class H cement	20.14	28.93	30.66
Class C fly ash	6.78	9.72	10.30
SiO ₂ flour	-	5.97	6.29
CaSO ₄ additive	2.46	3.41	3.62
NaCl	2.64	5.17	-
Plasticizer, Melment	0.98	-	-
Melgran 0	-	0.06	1.01
Defoamer	0.07	0.10	1.01
Deionized water	8.17	16.84	16.39
Sand	58.75	29.80	31.62

Table 2.5 Compositions of Formulations 82-030, 82-14 and 82-02 (Roy et al., 1983, as quoted by Roy et al., 1985).

Component (wt % of total)	Mixture		
	82-02	82-030	82-14
Class H cement	49.02	60.21	53.78
High lime fly ash	12.27	19.36	13.44
Gypseal	-	8.25	-
Low lime fly ash	12.25	-	13.44
Ohio fume	8.17	6.04	8.96
5- μ m Quartz	-	6.13	-
C 109 sand	89.87	-	98.59
NaCl	-	-	10.37
CaCl ₂	18.30	-	-
D-65	0.82	1.42	0.90
D-47	0.30	0.02	-
Citric acid	0.20	-	-
Water	23.00	25.88	25.21

Tepnarong (2012) studied the frictional shear strengths between cement grout and rock salt fractures by series of borehole push-out testing and direct shear testing. The salt specimens were prepared from the Maha Sarakham formation in the northeast of Thailand. The components of cement slurry were 700 g of Portland-pozzolan cement (type IP), 385 g of NaCl Saturated Brine, 20 g of anti-form agent and 3.5 g of liquid additive. The curing period for all push-out tests and direct shear tests was 3 days. According to the Coulomb criterion, the friction angles at the cement-salt interface were 70° and 69° for fracture and saw cut surfaces, respectively. The cohesion for the cement-salt fracture was averaged as 0.42 MPa.

The push-out test results showed significantly higher values of the frictional resistance at the interface than did the direct shear testing. The axial shear strength of the borehole cement seal was as high as 7.05 to 11.23 MPa. This was due to the effect of the Poisson's ratio which increased the normal (radial) stress at the cement-salt interface while the axial load was applied. The results suggested that the direct shear test might give an over conservative estimate of the shearing resistance between the salt and the cement seal.

Samaiklang and Fuenkajorn (2013) studied the mechanical and hydraulic performance of commercial grade cement grouts in rock fracture. The results were compared in terms of compressive strength, tensile strength, bond strength and push-out strength for against rock fracture. All grouts were prepared by mixing at the water-cement ratio of 0.60. The compressive strength after 28 day curing times was 25.77 ± 2.54 MPa and the average tensile strength was 2.80 ± 0.27 MPa. The bond strength test and push-out test results indicate that the bond strength between the cured grout and Phu Kradung sandstone fractures was varying from 1.03 to 2.53 MPa, and the push-out strength varying from 4.06 to 5.55 MPa.

Tepnarong and Deethouw (2014) studied the performance of sludge-mixed cement grouts for sealing boreholes in rock salt. The components of cement slurry were 700 g of Portland-pozzolan cement (type V) mixed with sludge, 700 g of NaCl saturated brine, 20 g of anti-form agent and 3.5 g of liquid additive. The results led to the selection of the most suitable ratio of sludge-mixed cement (S:C) for grouting in the rock salt. The compressive strength 28 day curing times was 9.58 ± 0.52 MPa. The highest compressive strength was from ratio of S:C = 5:10. The tensile strength was 1.99 ± 0.14 MPa. The highest bond strength was 7.49 MPa

2.5 Direct Shear Creep Test

Dieterich (1972) performed direct shear tests on greywacke, granite, quartzite and porous sandstone. His investigations focused on the relationships between the duration of stationary contact and the static friction coefficient of unfilled and gouge filled rock joints. Samples were prepared by sawing blocks with subsequent lapping to obtain flat and parallel slip surfaces of a required roughness. The static friction at the end of a desired interval was then measured by rapidly increasing the shear stress until the block moved. The time interval was between 1 sec and 24 hours and the normal stress was varied between 2 and 85 MPa. The results showed that the coefficient of static friction of joints was time independent for a clean rough joint surface while a joint with gouge exhibits a highly time-dependent behavior. Static friction increased with the time that adjacent blocks remain in stationary contact.

Lajtai and Gadi (1989) studied the time-dependence on friction in fractures planes. They performed direct shear tests on smooth, planar rock blocks of Lac du Bonnet granite. The test specimens were cut by diamond saw and ground to the required size with subsequent polishing of the shear surface. The normal load ranged from 0.2 to 8 MPa. No steady state displacement was observed in any of the tests. The frictional resistance in the tests increased with both displacement and time. The increase of the frictional resistance of an initially smooth and polished surface during continuing shearing displacement is due to wear. The results confirmed the findings by Dieterich (1972) that most likely creep was transient in rock joints under shear conditions that accumulate gouge fill.

Amadei and Curran (1982) conducted triaxial and direct shear tests on unfilled and clean rock joints under a variety of stress states and surface conditions.

The creep displacement in a discontinuity was a function of both the normal stress (σ_n) and the shear stress (τ_p) of the fracture. Under a constant normal stress, the creep deformation was expected to increase as the shear stress is increased and, for a constant shear stress, decreased if the normal stress is increased.

Yang and Cheng (2011) studied based on visco-elastic shear creep experimental results of shale with four various shear stress levels, Stationary (linear) shear creep model parameters have a strong time scale effect, which shows that the visco-elastic shear modulus G_2 of rock decreases but the visco-coefficient η_1 increases with increasing time. A non-stationary visco-elastic shear creep model is put forward to describe visco-elastic shear deformation behavior of rock by confirming the relation between stationary creep parameters G_2 , η_1 and time. The non-stationary shear creep model has a better agreement with experimental data than stationary shear creep model, but which is not very good for predicting long-term deformation behavior.

Saptono et al. (2012) a research of shear strength characteristics on rock samples of the predominant coal bearing strata such as sandstone which are obtained from Tutupan coal mines in South Kalimantan, Indonesia. The research includes the shear creep test with Generalized Kelvin model rheology approach with 15 x 15 cm and 25 x 25 cm sandstone samples size respectively. The research reveals that the long term strength of that sandstone is significantly lower than their peak strengths. It is also found that the Generalized Kelvin rheology model does fit to the rheology of these rock samples.

2.6 Permeability Properties of Rock Salt and Cement Grout

Stormont (1990) measured permeability of bedded rock salt from the vicinity of the tunnel is about 10^{-22} m² (or approximately 10^{-9} darcy). Whereas permeability of rock salt in adjacent to the wall of tunnel might be higher than 10^{-18} m² (or approximately 10^{-5} darcy). Later, Stormont and Deamen (1991) and Peach (1991) performed laboratory testing and the results confirmed that salt permeability could be higher than expected especially when rock salt was under anisotropic stress. Differential stress at a point can be high enough to cause micro-cracks to develop in rock salt. The direction of these micro-cracks was almost parallel to the major principal stress direction. Besides, permeability for air or liquid of bedded rock salt depended on stress magnitude and on the difference in magnitude of principal stresses in three directions at that point. Therefore, the difference in stress magnitude would be maximum at the walls of cavern or tunnel. Rock salt deformed in elastic that depended on time. At a state where the difference in the stress magnitude was high enough, cracks develops and cause higher permeability. Whereas for the salt at the point located far from the tunnel of cavern walls, the difference in principal stress magnitude was low and deformation was also low. Cracks might not develop in rock salt located far from the tunnel vicinity, and the permeability value was still as low as it had not been affected by the creation of the tunnel. Brodsky et al. (1998) studied rock salt permeability by using crushed rock salt with density of 0.85 to 0.90 g/cm³ and found that the permeability of intact rock specimens ranged from 10^{-15} to 10^{-12} m². Although permeability of the rock salt was relatively low, it could be higher as a result of mechanical damages such as crack developed during excavation of the cavern. Dale and Hurtado (1998) measured permeability around rock salt cavern and

found that cracks developed within a distance less than 3 m around the cavern and the permeability value was as low as 10^{-21} m^2

Wong et al (2011) measured permeability of cement-based materials using pore areas and perimeters from SEM images. The pore structure was idealized as a cubic lattice having pores of arbitrary size. The hydraulic conductance of each pore was applied to account for the random orientation of the image plane. A constriction factor was applied to account for variations in pore radius along the pore axis. Kirkpatrick's effective medium equation was then used to obtain an effective pore conductance, from which the macroscopic permeability was derived. The method was tested on forty-six pastes and mortars with different water-cement ratio, cement, age and sand constant. The permeability ranged from $3 \times 10^{-18} \text{ m}^2$ to $5.8 \times 10^{-16} \text{ m}^2$. Samaiklang and Fuenkajorn (2013) performed laboratory testing permeability of grouts are prepared by mixing at the water-cement ratio of 0.60 measured from the longitudinal flow test with constant heat was from 10^{-16} to 10^{-14} m^2 and decreased with curing time.

CHAPTER III

CEMENT GROUTS AND ROCK SALT SPECIMENS

PREPARATION

3.1 Cement Grout Preparation

The cement mixing for the borehole plugs and the direct shear testing prepared in this study is performed according to the API Specification No. 10 (American Petroleum Institute, 1986; Akgun and Daemen, 1997) by mixing cement with a salt (NaCl) saturated brine. The two types of cement used are Salt-bond II with low brine content (SBII) cement and Salt-bond II with high brine content (SBIH) cement. The components of cement slurry are commercial grade Portland cement mixed with chloride resistant agent, NaCl saturated brine, anti-form agent and a liquid additive including expansion. The brine is prepared by dissolving clean rock salt in distilled water.

Portland-pozzolan cement is chosen due to its low brine demand, sulfate resistance and widely used in construction industry (Figures 3.1). A liquid additive contributes to expansiveness of mixture. An anti-forming agent is used to decrease the air content of the cement slurry and to ease a control of cement slurry weight and volume. Table 3.1 gives the weight compositions of the mixtures.

3.1.1 Apparatus

Apparatus used in these preparation consist of:

- 1) Plastic scoop.

- 2) Digital weight scale (Capacity of 2,000 g).
- 3) Mixture (Kitchenaid 600 6QT model with maximum capacity of 5,000 cm³ and 10 speed control).
- 4) PVC molds and Rubber stopper.
- 5) Funnel and plastic tube.
- 6) Digital thermometer (HPI temp gun).
- 7) Silicon grease.

3.1.2 Procedure for preparing cement borehole plugs

- 1) Prepare the cement slurry at an ambient room temperature (28 to 34 °C) and relative room humidity not less than 50%.
- 2) Prepare saturated brine by chemically pure salt in distilled water into the Nalgene tank. Leave for a day to obtain saturated brine with a specific gravity of 1.18 at 32°C.
- 3) Place the saturated brine, liquid additive and anti-form agent into the mixing container. Add the cement to the brine-liquid additive-anti-form agent mixture in not more than 15 seconds (while the mixer speed remains on 2). After all the cement is added, continue mixing at speed 6 for an additional 3 minutes.
- 4) Place a rubber stopper into the borehole at the level where a 25 mm long, centered cement plug is to be located. Pour the cement slurry onto the rubber stopper with minimum time lag (in less than 30 seconds).
- 5) Pour cement through a funnel and plastic tube. Submerge the bottom end of the plastic tube in the slurry. Raise the funnel and

tube as the cement slurry level increases. Minimize turbulence as much as possible during pouring. Stop pouring when a 30 mm plug length is obtained.

- 6) Cure the cement plugs in salt specimens for 7 days, at atmospheric pressure and at a room temperature prior to initiating testing.
- 7) Grind the top end of the cement plug with a blind bit.

The cement slurry mixtures are poured and cured in 54 mm diameter PVC mold for the mechanical characterization test (Figures 3.2) and 100 mm diameter PVC mold for the permeability test are listed in Table 3.2 through 3.4. Figures 3.3 and 3.4 show some of the specimens prepared for mechanical characterization test and permeability test.



Figure 3.1 Bag of Portland-pozzolan cement 50 kg is used in this study.

Table 3.1 Weight composition of Salt-bond II cement (SBII and SBIH).

Composition of slurry (g)	SBII	SBIH
Portland-pozzolan cement, type IP	1000	1000
NaCl saturated brine	450	670
Liquid additive	10	10
Anti-form agent	10	10

Table 3.2 Specimen dimensions prepared for uniaxial compressive strength testing and elastic modulus measurement.

Cement Sample No.	Curing time (days)	Diameter (mm)	Length (mm)	L/D	Density (g/cm ³)
SBII-02-01-UCS-01	1	54.06	135.49	2.51	1.70
SBII-02-01-UCS-02		53.99	135.00	2.50	1.70
SBII-02-01-UCS-03		53.99	135.58	2.51	1.71
SBII-02-03-UCS-01	3	53.82	136.32	2.53	1.76
SBII-02-03-UCS-02		53.81	135.16	2.51	1.77
SBII-02-03-UCS-03		54.01	135.55	2.51	1.74
SBII-02-07-UCS-01	7	54.02	135.36	2.51	1.74
SBII-02-07-UCS-02		53.81	134.66	2.50	1.75
SBII-02-07-UCS-03		53.97	135.56	2.51	1.78
SBII-02-14-UCS-01	14	53.55	135.05	2.52	1.76
SBII-02-14-UCS-02		53.91	135.75	2.52	1.74
SBII-02-14-UCS-03		53.81	135.46	2.52	1.74
SBII-02-21-UCS-01	21	54.19	133.67	2.47	1.74
SBII-02-21-UCS-02		53.91	135.67	2.52	1.77
SBII-02-21-UCS-03		53.69	134.77	2.51	1.77
SBII-02-28-UCS-01	28	53.93	134.32	2.49	1.79
SBII-02-28-UCS-02		53.85	134.25	2.49	1.72
SBII-02-28-UCS-03		53.82	133.79	2.49	1.72
SBII-02-60-UCS-01	60	54.19	135.23	2.50	1.76
SBII-02-60-UCS-02		54.23	134.43	2.48	1.76
SBII-02-60-UCS-03		54.17	133.85	2.47	1.74

Table 3.2 Specimen dimensions prepared for uniaxial compressive strength testing and elastic modulus measurement (continued).

Cement Sample No.	Curing time (days)	Diameter (mm)	Length (mm)	L/D	Density (g/cm³)
SBIH-02-01-UCS-01	1	53.53	133.47	2.49	1.73
SBIH-02-01-UCS-02		54.03	133.64	2.47	1.72
SBIH-02-01-UCS-03		53.38	133.84	2.51	1.73
SBIH-02-03-UCS-01	3	54.09	135.03	2.50	1.73
SBIH-02-03-UCS-02		54.05	135.01	2.50	1.73
SBIH-02-03-UCS-03		53.95	134.85	2.50	1.71
SBIH-02-07-UCS-01	7	53.97	134.55	2.49	1.72
SBIH-02-07-UCS-02		53.80	134.31	2.50	1.73
SBIH-02-07-UCS-03		53.93	135.21	2.51	1.73
SBIH-02-14-UCS-01	14	53.55	135.51	2.53	1.73
SBIH-02-14-UCS-02		53.82	136.47	2.54	1.72
SBIH-02-14-UCS-03		53.61	135.82	2.53	1.72
SBIH-02-21-UCS-01	21	53.81	134.89	2.51	1.72
SBIH-02-21-UCS-02		54.33	134.13	2.47	1.71
SBIH-02-21-UCS-03		53.53	134.20	2.51	1.75
SBIH-02-28-UCS-01	28	53.61	134.11	2.50	1.73
SBIH-02-28-UCS-02		53.73	133.99	2.49	1.74
SBIH-02-28-UCS-03		54.63	135.03	2.47	1.73
SBIH-02-60-UCS-01	60	54.16	135.91	2.51	1.69
SBIH-02-60-UCS-02		53.91	135.19	2.51	1.71
SBIH-02-60-UCS-03		54.11	133.71	2.47	1.70

Table 3.3 Specimen dimensions prepared for Brazilian tensile strength testing.

Cement Sample No.	Curing time (days)	Diameter (mm)	Length (mm)	L/D	Density (g/cm ³)
SBII-02-01-BZ-01	1	54.21	26.29	0.48	1.67
SBII-02-01-BZ-02		54.05	26.34	0.49	1.69
SBII-02-01-BZ-03		53.96	26.83	0.50	1.71
SBII-02-01-BZ-04		54.22	27.59	0.51	1.70
SBII-02-01-BZ-05		54.09	27.21	0.50	1.68
SBII-02-03-BZ-01	3	53.83	26.34	0.49	1.74
SBII-02-03-BZ-02		53.89	26.50	0.49	1.76
SBII-02-03-BZ-03		54.10	25.79	0.48	1.74
SBII-02-03-BZ-04		54.31	25.83	0.48	1.73
SBII-02-03-BZ-05		53.57	25.77	0.48	1.76
SBII-02-07-BZ-01	7	53.99	27.80	0.51	1.71
SBII-02-07-BZ-02		53.90	26.49	0.49	1.71
SBII-02-07-BZ-03		53.91	28.05	0.52	1.72
SBII-02-07-BZ-04		53.81	26.85	0.50	1.70
SBII-02-07-BZ-05		53.82	27.06	0.50	1.75
SBII-02-14-BZ-01	14	53.93	27.13	0.50	1.73
SBII-02-14-BZ-02		53.71	27.92	0.52	1.82
SBII-02-14-BZ-03		53.98	28.63	0.53	1.79
SBII-02-14-BZ-04		53.93	27.51	0.51	1.78
SBII-02-14-BZ-05		53.91	28.21	0.52	1.79
SBII-02-21-BZ-01	21	53.43	28.51	0.53	1.78
SBII-02-21-BZ-02		53.91	27.83	0.52	1.74
SBII-02-21-BZ-03		53.84	27.16	0.50	1.71
SBII-02-21-BZ-04		54.04	28.61	0.53	1.75
SBII-02-21-BZ-05		53.94	27.61	0.51	1.71
SBII-02-28-BZ-01	28	53.54	28.81	0.54	1.75
SBII-02-28-BZ-02		53.49	27.02	0.51	1.76
SBII-02-28-BZ-03		53.41	27.02	0.51	1.76
SBII-02-28-BZ-04		53.55	26.57	0.50	1.73
SBII-02-28-BZ-05		53.61	27.59	0.51	1.74

Table 3.3 Specimen dimensions prepared for Brazilian tensile strength testing
(continued).

Cement Sample No.	Curing time (days)	Diameter (mm)	Length (mm)	L/D	Density (g/cm ³)
SBII-02-60-BZ-01	60	54.11	28.71	0.53	1.75
SBII-02-60-BZ-02		54.00	27.35	0.51	1.76
SBII-02-60-BZ-03		54.02	27.62	0.51	1.76
SBII-02-60-BZ-04		54.11	27.45	0.51	1.73
SBII-02-60-BZ-05		54.05	28.80	0.53	1.75
SBIH-02-01-BZ-01	1	53.54	27.31	0.51	1.76
SBIH-02-01-BZ-02		53.75	28.23	0.53	1.76
SBIH-02-01-BZ-03		54.15	26.38	0.49	1.75
SBIH-02-01-BZ-04		53.61	26.80	0.50	1.76
SBIH-02-01-BZ-05		53.51	27.03	0.51	1.75
SBIH-02-03-BZ-01	3	54.19	28.30	0.52	1.76
SBIH-02-03-BZ-02		54.23	27.33	0.50	1.72
SBIH-02-03-BZ-03		54.15	28.40	0.52	1.71
SBIH-02-03-BZ-04		54.12	25.89	0.48	1.72
SBIH-02-03-BZ-05		54.31	27.13	0.50	1.69
SBIH-02-07-BZ-01	7	53.93	26.61	0.49	1.72
SBIH-02-07-BZ-02		53.56	27.39	0.51	1.72
SBIH-02-07-BZ-03		54.43	27.31	0.50	1.72
SBIH-02-07-BZ-04		53.93	28.30	0.52	1.71
SBIH-02-07-BZ-05		53.72	26.21	0.49	1.73
SBIH-02-14-BZ-01	14	53.71	27.41	0.51	1.74
SBIH-02-14-BZ-02		53.31	27.11	0.51	1.79
SBIH-02-14-BZ-03		53.32	26.78	0.50	1.77
SBIH-02-14-BZ-04		53.55	27.53	0.51	1.76
SBIH-02-14-BZ-05		53.75	26.89	0.50	1.75
SBIH-02-21-BZ-01	21	53.81	27.63	0.51	1.76
SBIH-02-21-BZ-02		54.38	27.33	0.50	1.71
SBIH-02-21-BZ-03		53.85	27.43	0.51	1.72
SBIH-02-21-BZ-04		54.13	28.19	0.52	1.68
SBIH-02-21-BZ-05		54.21	27.81	0.51	1.69

Table 3.3 Specimen dimensions prepared for Brazilian tensile strength testing
(continued).

Cement Sample No.	Curing time (days)	Diameter (mm)	Length (mm)	L/D	Density (g/cm ³)
SBIH-02-28-BZ-01	28	53.65	26.55	0.49	1.69
SBIH-02-28-BZ-02		53.63	28.77	0.54	1.71
SBIH-02-28-BZ-03		53.55	27.19	0.51	1.74
SBIH-02-28-BZ-04		53.71	27.82	0.52	1.68
SBIH-02-28-BZ-05		53.53	28.21	0.53	1.72
SBIH-02-60-BZ-01	60	54.11	27.61	0.51	1.70
SBIH-02-60-BZ-02		54.14	27.73	0.51	1.74
SBIH-02-60-BZ-03		54.20	28.11	0.52	1.72
SBIH-02-60-BZ-04		54.14	28.31	0.52	1.75
SBIH-02-60-BZ-05		54.04	27.22	0.50	1.71

Table 3.4 Cement grout specimen prepared for long-term permeability testing.

Cement Sample No.	Diameter (mm)	Length (mm)	L/D	Density (g/cm ³)
SBII-04-P	98.16	104.79	1.07	1.76
SBIH-04-P	98.13	100.42	1.02	1.74

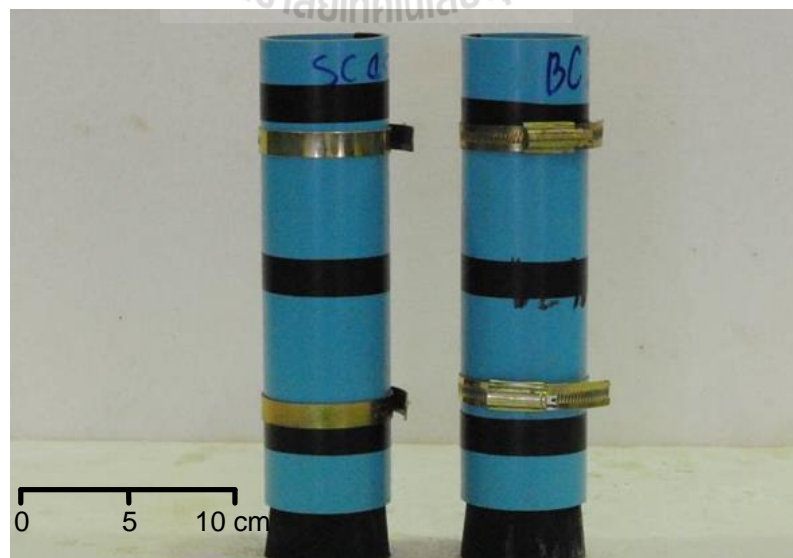


Figure 3.2 PVC molds with curing cement mixture.

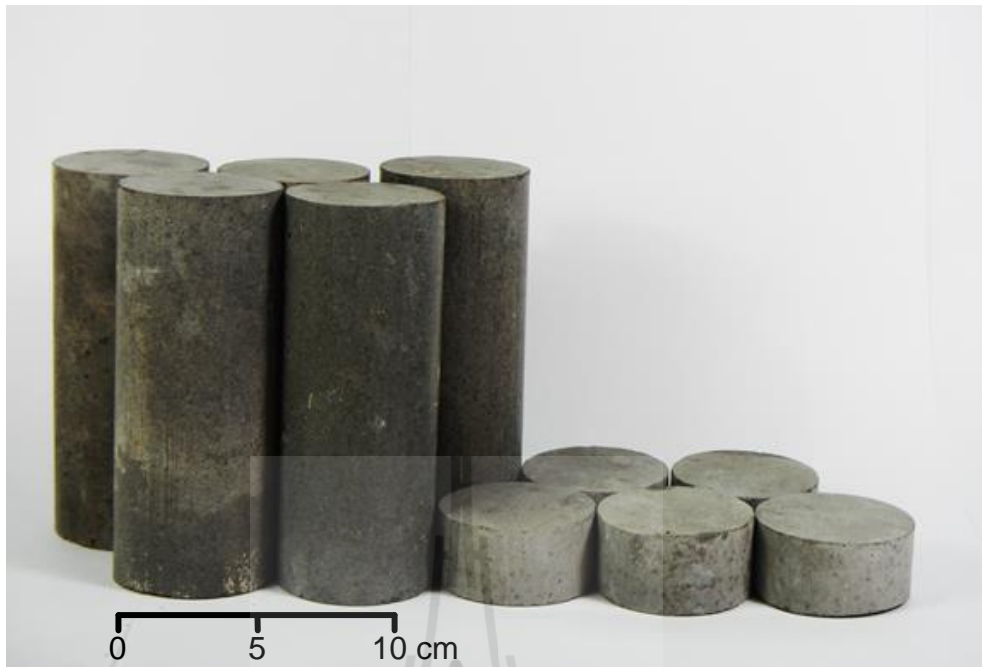


Figure 3.3 Some of specimens prepared for mechanical characterization testing.



Figure 3.4 Cement grout cylinders within the PVC mold for permeability testing.

3.2 Rock Salt Specimens

100 mm diameter core samples of rock salt are donated by Asean Potash Mining Company. They are collected from a borehole number of KB-09 located in Bumnetnarong district, Chaiyaphum province. All samples are obtained from the Middle Salt member at depths between 70 m and 130 m of the Khorat basin. The petrographic properties of the tested cores are as follows. The salt crystals are tightly interlocked. The white and clear halite change to pale, medium and dark honey when the depths increase. The diameters of milky white halite range from 0.1 to 0.3 cm, showing flow texture. Smoky dark halite is associated with anhydrite. The large recrystallized glassy halite is found interlayered with the honey halite. The associated minerals include local occurrence of sylvite and carnallite. Some large crystals ranging from 2.0 to 5.0 cm are locally occurred. (Tepnarong, 2012).

Sample preparation are followed the ASTM D4543 standard practice, as much as practical. Specimens are prepared for the direct shear strength tests and the push-out tests with length of 100 mm are listed in Table 3.5 and 3.6. The cylindrical push-out specimens are drilled with 25 mm diameter holes perpendicular to the bottom sample surfaces (Figure 3.5 and 3.6). The saw cut surfaces are prepared for the direct shear testing (Figure 3.7 and 3.8). After preparation, the specimens are labeled and wrapped with a plastic film. The specimen designation is identified.

Table 3.5 Depth and specimen dimensions of rock salt and cement plugs prepared for push-out testing.

Specimen No.	Depth (m)	Rock salt		Cement plugs	
		D _o (mm)	L (mm)	D _i (mm)	L _c (mm)
SBIH-04-07-PO-01	116.150-116.250	98.42	100.39	25.81	28.71
SBIH-04-07-PO-02	121.140-121.241	100.21	100.53	25.68	32.67
SBIH-04-07-PO-03	73.950-74.054	100.01	104.02	25.22	28.90
SBIH-04-07-PO-04	73.700-73.801	100.18	101.27	25.63	29.11
SBIH-04-07-PO-05	73.550-73.650	100.25	100.07	26.35	30.17
SBIH-04-07-PO-06	119.000-119.102	102.33	101.23	26.23	28.55

Table 3.6 Depth and specimen dimensions of rock salt prepared for direct shear testing.

Specimen No.	Depth (m)	Diameter (mm)	Length (mm)	Density (g/cm ³)
SBIH-04-07-DS-01	83.038-83.078	100.97	40.12	2.05
SBIH-04-07-DS-02	121.000-121.037	100.60	37.28	2.07
SBIH-04-07-DS-03	121.037-121.079	100.49	42.10	2.07
SBIH-04-07-DS-04	121.079-121.120	100.49	41.36	2.06
SBIH-04-07-DS-05	121.120-121.160	100.61	41.14	2.06
SBIH-04-07-DS-06	129.590-129.659	100.29	69.00	2.05
SBIH-04-07-DS-07	116.000-116.071	100.73	70.55	2.18
SBIH-04-07-DS-08	71.940-72.005	100.10	64.51	2.19
SBIH-04-07-DS-09	73.630-73.700	100.13	69.80	2.16
SBIH-04-07-DS-10	77.040-77.110	101.17	70.21	2.18



Figure 3.5 Push-out test specimens is drilled with 25 mm diameter holes perpendicular to the bottom.



Figure 3.6 Some of rock salt specimens prepared for the push-out testing.



Figure 3.7 Salt core is dry-cut by a cutting machine.

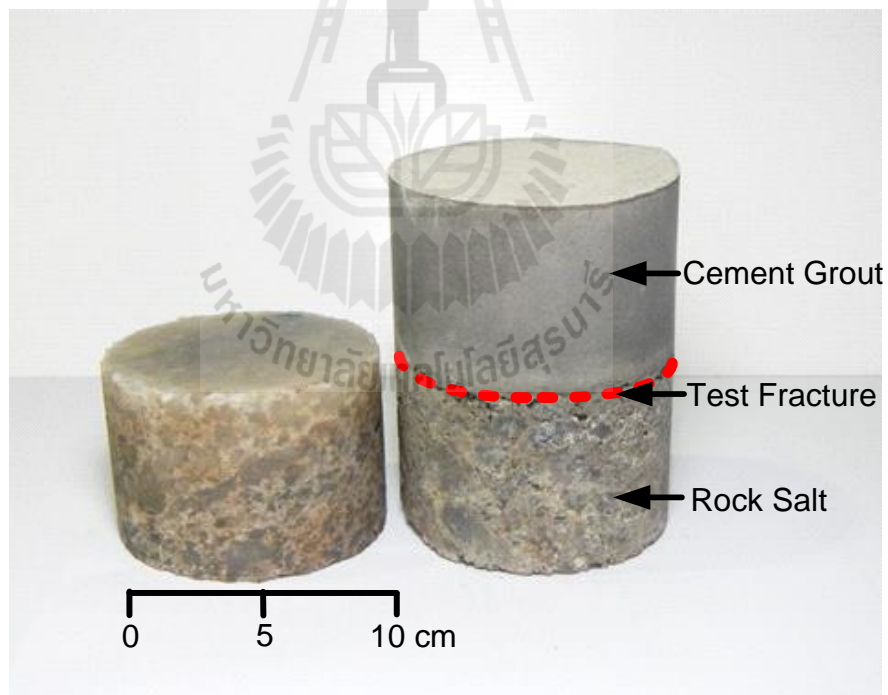


Figure 3.8 Saw cut surfaces and cement-rock salt interface are prepared for the direct shear testing.

CHAPTER IV

LABORATORY TESTING

4.1 Introduction

The objective of the laboratory testing is to study the mechanical and hydraulic performance assessment of cement sealing in rock salt. This chapter describes the method and results of the laboratory testing. The tests are divided into four groups including 1) basic mechanical properties tests of cement grout, 2) push-out tests, 3) direct shear tests, and 4) permeability tests of cement grout.

4.2 Basic Mechanical Properties Tests of Cement Grout

The basic mechanical properties test of cement grout include viscosity and slurry density of cement grout, uniaxial compressive strength (σ_c), elastic modulus (E) and Brazilian tensile strength (σ_B).

4.2.1 Viscosity and slurry density of cement grout

The cement grout preparation follows the ASTM (C938) standard practice a using a Hobart type laboratory mixer.

- 1) The cement slurry mixtures are poured in beaker 500 ml.
- 2) Weighing of cement slurry mixtures in beaker and record.
- 3) Calculate the density of cement slurry.
- 4) Install beaker of cement slurry mixtures in viscometer machine.
- 5) Measure the viscosity of cement slurry mixtures and record.

The density test follows the ASTM (D854) standard practice. The viscosity test follows the ASTM (D2196) standard practice is measured with Brookfield® viscometer model RV (Figure 4.1). The viscosity and slurry density test results in term of the specific gravity and viscosity. The weight of cement slurry is used to determine the flowability after mixed during setting time. Table 4.1 shows the result of viscosity and slurry density of cement slurry.



Figure 4.1 Brookfield® viscometer model RV (ASTM D2196).

Table 4.1 Viscosity and slurry density of cement slurry.

Specimen type	Temperature (°C)		Slurry density (g/cm ³)	Dynamic viscosity (Pa.s)	Kinematic viscosity (10 ⁻³ m ² /s)
	Room	Slurry			
SBII-1	32.5	32.0	2.00	32.50	16.22
SBII-2	32.0	31.0	2.01	35.00	17.43
SBII-3	32.5	32.0	2.00	35.00	17.53
SBII-4	33.0	32.5	1.98	38.00	19.20
SBII-5	33.0	32.5	1.99	32.25	16.24
Average			1.99±0.01	34.55±2.33	17.32±1.22
SBIH-1	32.5	32.0	1.75	4.90	2.80
SBIH-2	32.5	32.0	1.75	4.85	2.78
SBIH-3	32.5	32.0	1.74	4.10	2.36
SBIH-4	34.0	32.5	1.75	4.78	2.74
SBIH-5	34.0	32.0	1.77	4.00	2.26
Average			1.75±0.01	4.53±0.44	2.59±0.26

4.2.2 Uniaxial compressive strength tests

Preparation of these specimens follows, as much as practical, the ASTM D7012, C938 and C39. Specimens of 54 mm diameter cylindrical cement specimens with length to diameter ratios between 2.5 and 3.0 are prepared by curing cement pastes in PVC molds for 1, 3, 7, 14, 21, 28 and 60 days. The cement grouts are loaded at the constant rate of 0.1-0.5 MPa/s until failure. The axial displacements are monitored by displacement dial gauges (Figure 4.2).

The results of uniaxial compressive strength test and elastic modulus measurements are shown in Table 4.2 and 4.3. Figure 4.3 plot the uniaxial compressive strength as a function of curing time. The curing time increases the uniaxial compressive strength and the elastic modulus of cement grout increases.

4.2.3 Brazilian tensile strength tests

The objective of the Brazilian tensile strength tests is to determine the indirect tensile strength of cement grouts. The Brazilian tensile strength tests are performed in accordance with ASTM standard (D3967) and ISRM suggested method (Brown, 1981). Specimens of 54 mm diameter cylindrical cement specimens with length to diameter ratios is 0.5 are prepared by curing cement pastes in PVC molds for 1, 3, 7, 14, 21, 28 and 60 days. The test is performed by increasing the axial loaded at the constant rate of 0.1-0.5 MPa/s to cement grout specimen until failure occurred (Figure 4.4).

The results of Brazilian tensile strength tests are shown in Table 4.4 and 4.5. Figure 4.5 plot the Brazilian tensile strength as a function of curing time. The curing time increases the Brazilian tensile strength of cement grout increases. The average and standard deviation of characterization tests are shown in Table 4.6.

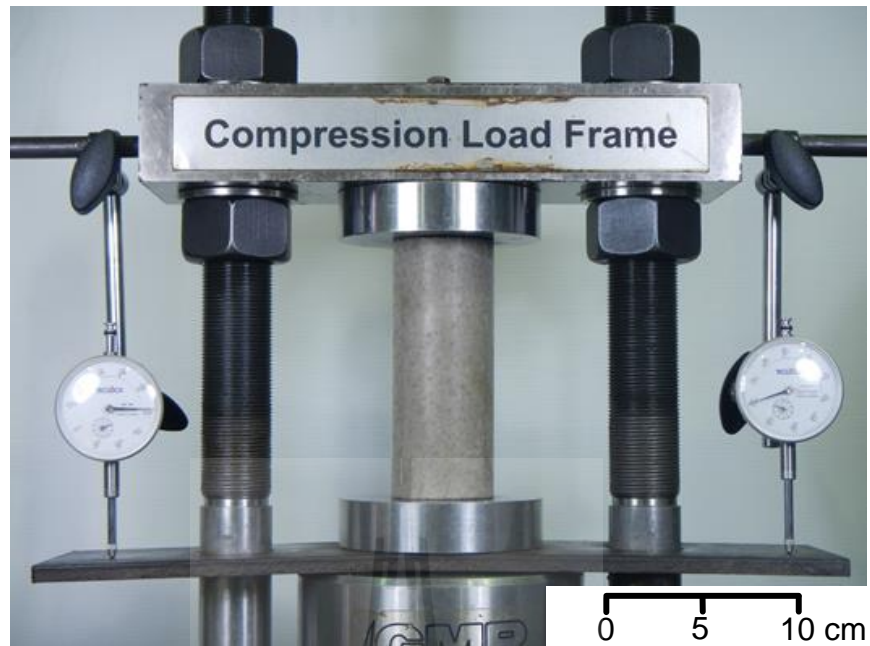


Figure 4.2 Uniaxial compressive strength tests.

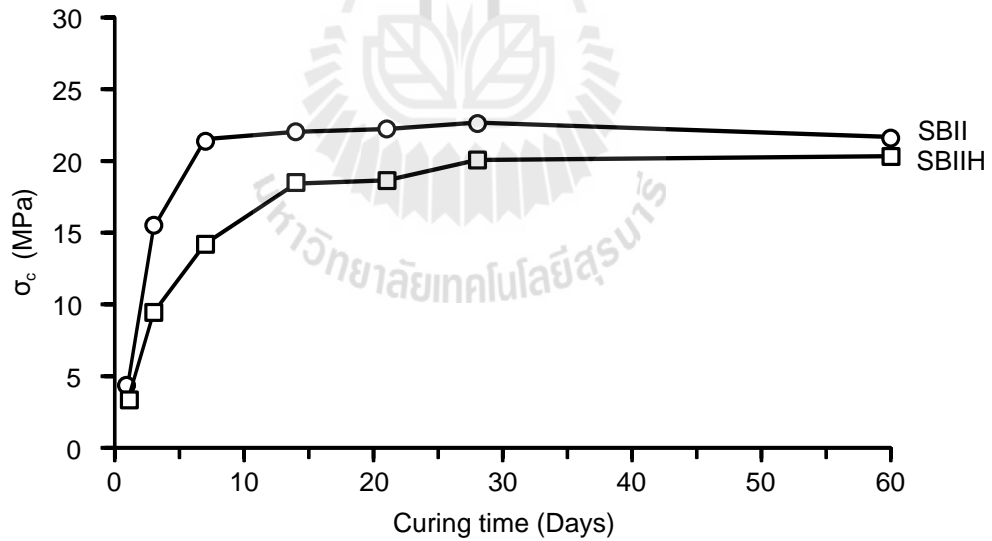


Figure 4.3 Uniaxial compressive strengths (σ_c) as a function of curing time.

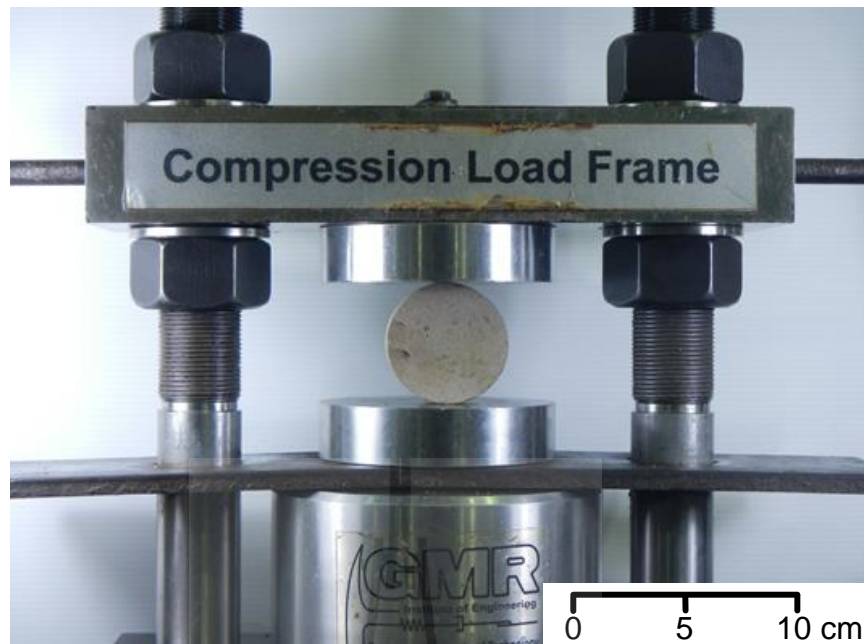


Figure 4.4 Brazilian tensile strength tests.

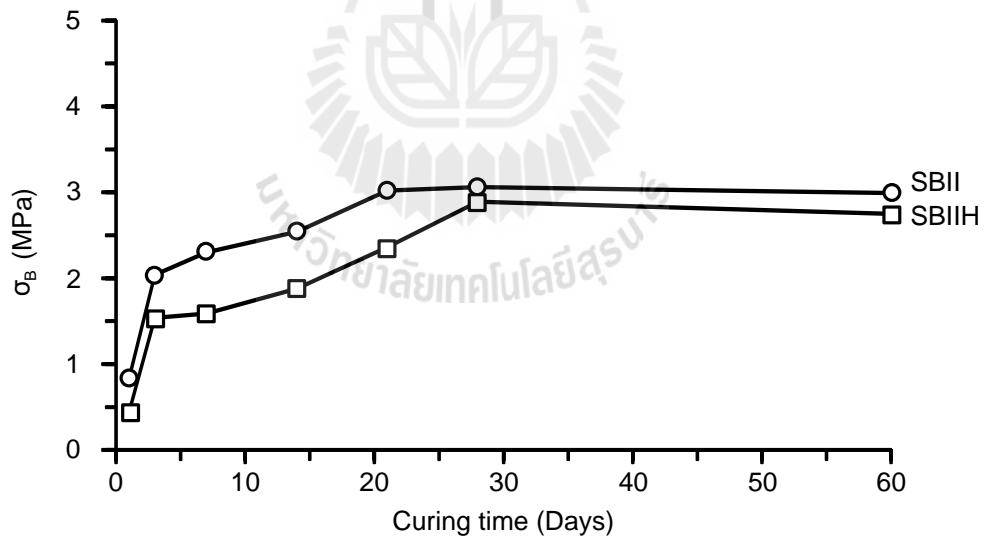


Figure 4.5 Brazilian tensile strengths (σ_B) as a function of curing time.

Table 4.2 Uniaxial compressive strength (σ_c) and elastic modulus (E) of Salt-bond II cement with a low brine content (SBII).

Specimen type	Curing time (days)	L/D	Density (g/cm ³)	σ_c (MPa)		E (GPa)	
SBII-02-01-UCS-01	1	2.51	1.70	4.36	4.36 ± 0.01	1.26	1.20 ± 0.05
SBII-02-01-UCS-02		2.50	1.70	4.37		1.18	
SBII-02-01-UCS-03		2.51	1.71	4.37		1.17	
SBII-02-03-UCS-01	3	2.53	1.76	16.48	15.35 ± 1.10	2.60	2.59 ± 0.06
SBII-02-03-UCS-02		2.51	1.77	14.29		2.65	
SBII-02-03-UCS-03		2.51	1.74	15.28		2.53	
SBII-02-07-UCS-01	7	2.51	1.74	22.91	21.52 ± 1.59	3.03	2.70 ± 0.30
SBII-02-07-UCS-02		2.50	1.75	19.79		2.42	
SBII-02-07-UCS-03		2.51	1.78	21.85		2.65	
SBII-02-14-UCS-01	14	2.52	1.76	19.98	22.03 ± 2.85	1.79	1.92 ± 0.14
SBII-02-14-UCS-02		2.52	1.74	20.81		1.90	
SBII-02-14-UCS-03		2.52	1.74	25.29		2.06	
SBII-02-21-UCS-01	21	2.47	1.74	27.10	22.23 ± 4.38	2.24	1.70 ± 0.47
SBII-02-21-UCS-02		2.52	1.77	18.62		1.34	
SBII-02-21-UCS-03		2.51	1.77	20.98		1.52	
SBII-02-28-UCS-01	28	2.49	1.79	27.36	22.67 ± 4.10	2.47	2.02 ± 0.40
SBII-02-28-UCS-02		2.49	1.72	20.85		1.71	
SBII-02-28-UCS-03		2.49	1.72	19.78		1.88	
SBII-02-60-UCS-01	60	2.50	1.76	19.51	21.68 ± 1.90	1.83	1.87 ± 0.29
SBII-02-60-UCS-02		2.48	1.76	23.81		2.18	
SBII-02-60-UCS-03		2.47	1.74	21.70		1.60	

Table 4.3 Uniaxial compressive strength (σ_c) and elastic modulus (E) of Salt-bond II cement with a high brine content (SBIH).

Specimen type	Curing time (days)	L/D	Density (g/cm ³)	σ_c (MPa)		E (GPa)	
SBIH-02-01-UCS-01	1	2.49	1.73	3.33	3.32 ± 0.04	0.84	0.92 ± 0.10
SBIH-02-01-UCS-02		2.47	1.72	3.27		1.03	
SBIH-02-01-UCS-03		2.51	1.73	3.35		0.88	
SBIH-02-03-UCS-01	3	2.50	1.73	8.70	9.45 ± 1.25	1.21	1.32 ± 0.19
SBIH-02-03-UCS-02		2.50	1.73	10.89		1.53	
SBIH-02-03-UCS-03		2.50	1.71	8.75		1.20	
SBIH-02-07-UCS-01	7	2.49	1.72	14.21	14.24 ± 2.16	2.26	1.25 ± 0.12
SBIH-02-07-UCS-02		2.50	1.73	12.10		2.12	
SBIH-02-07-UCS-03		2.51	1.73	16.42		2.36	
SBIH-02-14-UCS-01	14	2.53	1.73	19.98	18.42 ± 2.53	1.95	1.64 ± 0.51
SBIH-02-14-UCS-02		2.54	1.72	19.78		1.87	
SBIH-02-14-UCS-03		2.53	1.72	15.51		1.05	
SBIH-02-21-UCS-01	21	2.51	1.72	17.59	18.64 ± 1.23	1.28	1.29 ± 0.01
SBIH-02-21-UCS-02		2.47	1.71	18.33		1.30	
SBIH-02-21-UCS-03		2.51	1.75	20.00		1.29	
SBIH-02-28-UCS-01	28	2.50	1.73	24.36	20.06 ± 3.82	2.44	1.79 ± 0.58
SBIH-02-28-UCS-02		2.49	1.74	18.75		1.35	
SBIH-02-28-UCS-03		2.47	1.73	17.07		1.58	
SBIH-02-60-UCS-01	60	2.51	1.69	19.53	20.34 ± 3.42	1.91	1.87 ± 0.38
SBIH-02-60-UCS-02		2.51	1.71	24.09		2.23	
SBIH-02-60-UCS-03		2.47	1.70	17.40		1.47	

Table 4.4 Summary of the Brazilian tensile strength tests (σ_B) of Salt-bond II cement with a low brine content (SBII).

Specimen type	Curing time (days)	L/D	Density (g/cm ³)	σ_B (MPa)
SBII-02-01-BZ-01	1	0.48	1.67	0.89
SBII-02-01-BZ-02		0.49	1.69	0.89
SBII-02-01-BZ-03		0.50	1.71	0.77
SBII-02-01-BZ-04		0.51	1.70	0.85
SBII-02-01-BZ-05		0.50	1.68	0.76
SBII-02-03-BZ-01	3	0.49	1.74	2.02
SBII-02-03-BZ-02		0.49	1.76	1.89
SBII-02-03-BZ-03		0.48	1.74	2.17
SBII-02-03-BZ-04		0.48	1.73	2.04
SBII-02-03-BZ-05		0.48	1.76	2.07
SBII-02-07-BZ-01	7	0.51	1.71	2.33
SBII-02-07-BZ-02		0.49	1.71	2.56
SBII-02-07-BZ-03		0.52	1.72	2.00
SBII-02-07-BZ-04		0.50	1.70	2.42
SBII-02-07-BZ-05		0.50	1.75	2.18
SBII-02-14-BZ-01	14	0.50	1.73	2.94
SBII-02-14-BZ-02		0.52	1.82	2.55
SBII-02-14-BZ-03		0.53	1.79	2.47
SBII-02-14-BZ-04		0.51	1.78	2.57
SBII-02-14-BZ-05		0.52	1.79	2.20
SBII-02-21-BZ-01	21	0.53	1.78	3.13
SBII-02-21-BZ-02		0.52	1.74	2.54
SBII-02-21-BZ-03		0.50	1.71	2.83
SBII-02-21-BZ-04		0.53	1.75	3.19
SBII-02-21-BZ-05		0.51	1.71	3.42
SBII-02-28-BZ-01	28	0.54	1.75	2.68
SBII-02-28-BZ-02		0.51	1.76	2.86
SBII-02-28-BZ-03		0.51	1.76	3.53
SBII-02-28-BZ-04		0.50	1.73	3.02
SBII-02-28-BZ-05		0.51	1.74	3.23
SBII-02-60-BZ-01	60	0.53	1.75	2.87
SBII-02-60-BZ-02		0.51	1.76	2.80
SBII-02-60-BZ-03		0.51	1.76	3.09
SBII-02-60-BZ-04		0.51	1.73	3.21
SBII-02-60-BZ-05		0.53	1.75	2.96

Table 4.5 Summary of the Brazilian tensile strength tests (σ_B) of Salt-bond II cement with a high brine content (SBIIH).

Specimen type	Curing time (days)	L/D	Density (g/cm^3)	σ_B (MPa)
SBIIH-02-01-BZ-01	1	0.51	1.76	0.44±0.01
SBIIH-02-01-BZ-02		0.53	1.76	
SBIIH-02-01-BZ-03		0.49	1.75	
SBIIH-02-01-BZ-04		0.50	1.76	
SBIIH-02-01-BZ-05		0.51	1.75	
SBIIH-02-03-BZ-01	3	0.52	1.76	1.54±0.06
SBIIH-02-03-BZ-02		0.50	1.72	
SBIIH-02-03-BZ-03		0.52	1.71	
SBIIH-02-03-BZ-04		0.48	1.72	
SBIIH-02-03-BZ-05		0.50	1.69	
SBIIH-02-07-BZ-01	7	0.49	1.72	1.59±0.08
SBIIH-02-07-BZ-02		0.51	1.72	
SBIIH-02-07-BZ-03		0.50	1.72	
SBIIH-02-07-BZ-04		0.52	1.71	
SBIIH-02-07-BZ-05		0.49	1.73	
SBIIH-02-14-BZ-01	14	0.51	1.74	1.88±0.13
SBIIH-02-14-BZ-02		0.51	1.79	
SBIIH-02-14-BZ-03		0.50	1.77	
SBIIH-02-14-BZ-04		0.51	1.76	
SBIIH-02-14-BZ-05		0.50	1.75	
SBIIH-02-21-BZ-01	21	0.51	1.76	2.36±0.28
SBIIH-02-21-BZ-02		0.50	1.71	
SBIIH-02-21-BZ-03		0.51	1.72	
SBIIH-02-21-BZ-04		0.52	1.68	
SBIIH-02-21-BZ-05		0.51	1.69	
SBIIH-02-28-BZ-01	28	0.49	1.69	2.89±0.19
SBIIH-02-28-BZ-02		0.54	1.71	
SBIIH-02-28-BZ-03		0.51	1.74	
SBIIH-02-28-BZ-04		0.52	1.68	
SBIIH-02-28-BZ-05		0.53	1.72	
SBIIH-02-60-BZ-01	60	0.51	1.70	2.75±0.18
SBIIH-02-60-BZ-02		0.51	1.74	
SBIIH-02-60-BZ-03		0.52	1.72	
SBIIH-02-60-BZ-04		0.52	1.75	
SBIIH-02-60-BZ-05		0.50	1.71	

Table 4.6 Summary of the uniaxial compressive strength (σ_c) tests, elastic modulus (E) measurements and Brazilian tensile strength tests (σ_B) of cement plugs.

Specimen age (days)	σ_c (MPa)		E (GPa)		σ_B (MPa)	
	SBI	SBIH	SBI	SBIH	SBI	SBIH
1	4.36±0.01	3.32±0.04	0.92±0.10	0.92±0.10	0.83±0.07	0.44±0.01
3	15.35±1.10	9.45±1.25	1.32±0.19	1.32±0.19	2.04±0.10	1.54±0.06
7	21.52±1.59	14.24±2.16	1.25±0.12	1.25±0.12	2.30±0.22	1.59±0.08
14	22.03±2.85	18.42±2.53	1.64±0.51	1.64±0.51	2.54±0.26	1.88±0.13
21	22.23±4.38	18.64±1.23	1.29±0.01	1.29±0.01	3.02±0.34	2.36±0.28
28	22.67±4.10	20.06±3.82	1.79±0.58	1.79±0.58	3.06±0.33	2.89±0.19
60	21.68±1.90	20.34±3.42	1.87±0.38	1.87±0.38	2.99±0.17	2.75±0.18

4.3 Push-out test

The objective of this test is to determine the axial mechanical strength and long-term deformation of borehole plugs in rock salt core through push-out tests. The curing period for push-out tests is 7 days. Figure 4.6 shows the schematic drawing of the push-out test setup. A cylindrical steel rod applies an axial load to a cement plug. The top and bottom displacement of the borehole plug are measured by dial gages. The axial load is measured by a load gage of hydraulic pump. The displacement is measured manually by dial gages with a resolution of 0.025 mm. A loading frame with a hydraulic cylinder applies the load. The machine has a capacity of 50 kN with a resolution of 0.5 kN.

Figure 4.7 shows the push-out test setup. A salt cylinder in PVC molds with cement plug is centered on the square platen. A steel cylinder of slightly smaller diameter than the plug is centered and transmits the load on top of the plug. The specimen is loaded under constant stress rate of 0.1 MPa/s. The load and top and bottom plug displacements are recorded manually at 10 seconds intervals until sliding occurs.

The bond strength or the average shear stress (τ_{av}) distribution induced by push-out test loading along the rock salt-cement plug interface can be calculated by the following equation (Stormont and Daeman, 1983):

$$\tau_{av} = F / \pi D_i L_c \quad (4.1)$$

where F is the failure load, D_i is the plug diameter and L_c is the plug length. The dimensions of salt cylinder and the bond strength of cement plugs are summarized in Table 4.7.

Figure 4.8 plots the applied shear stress as a function of the top and bottom plug displacements. The bottom plug displacements are small compared to the top axial displacements prior to bond failure. Upon a plug slip, the difference between the top and the bottom plug displacements decrease most probably due to stress relief caused by slip along the interface. Rock bridges fail at the bond strength (τ_{av}) is 5.05 MPa. Figure 4.9 shows sample no.SBIIIH-04-07-PO-01 which is cut along the axis after failure. The thick cement residue on the borehole walls above the (slipped) cement plug and absence of dissolution indicate good a bonding.

The push-out tests are performed on cement plugs with a series of relatively long curing time with a constant shear stress. Figure 4.10 plots the top plug displacements (δ_T) as a function of time with a various constant shear stress. The results show an instantaneous elastic strain and top plug displacements expected to increase as the shear stress is increased.

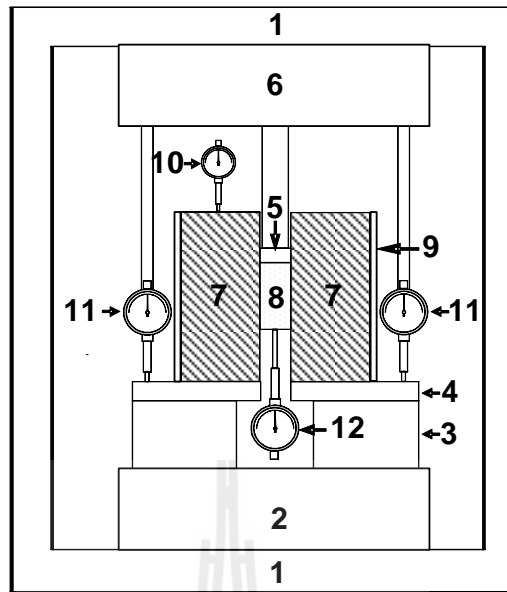


Figure 4.6 Schematic drawing of the push-out test setup, 1.Loading frame; 2.Hydraulic cylinder; 3.Steel plate with a slit; 4.Square steel plate; 5.Axial bar and steel cylinder; 6.Square steel plate frame; 7.Rock salt sample; 8.Cement grout plug; 9.PVC mold; 10., 11. and 12.Dial gages.

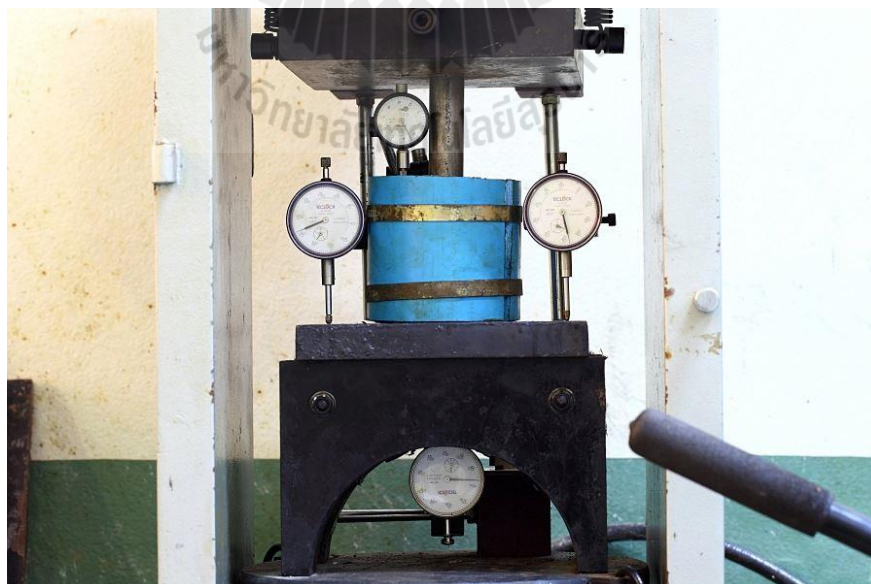


Figure 4.7 The push-out test setup.

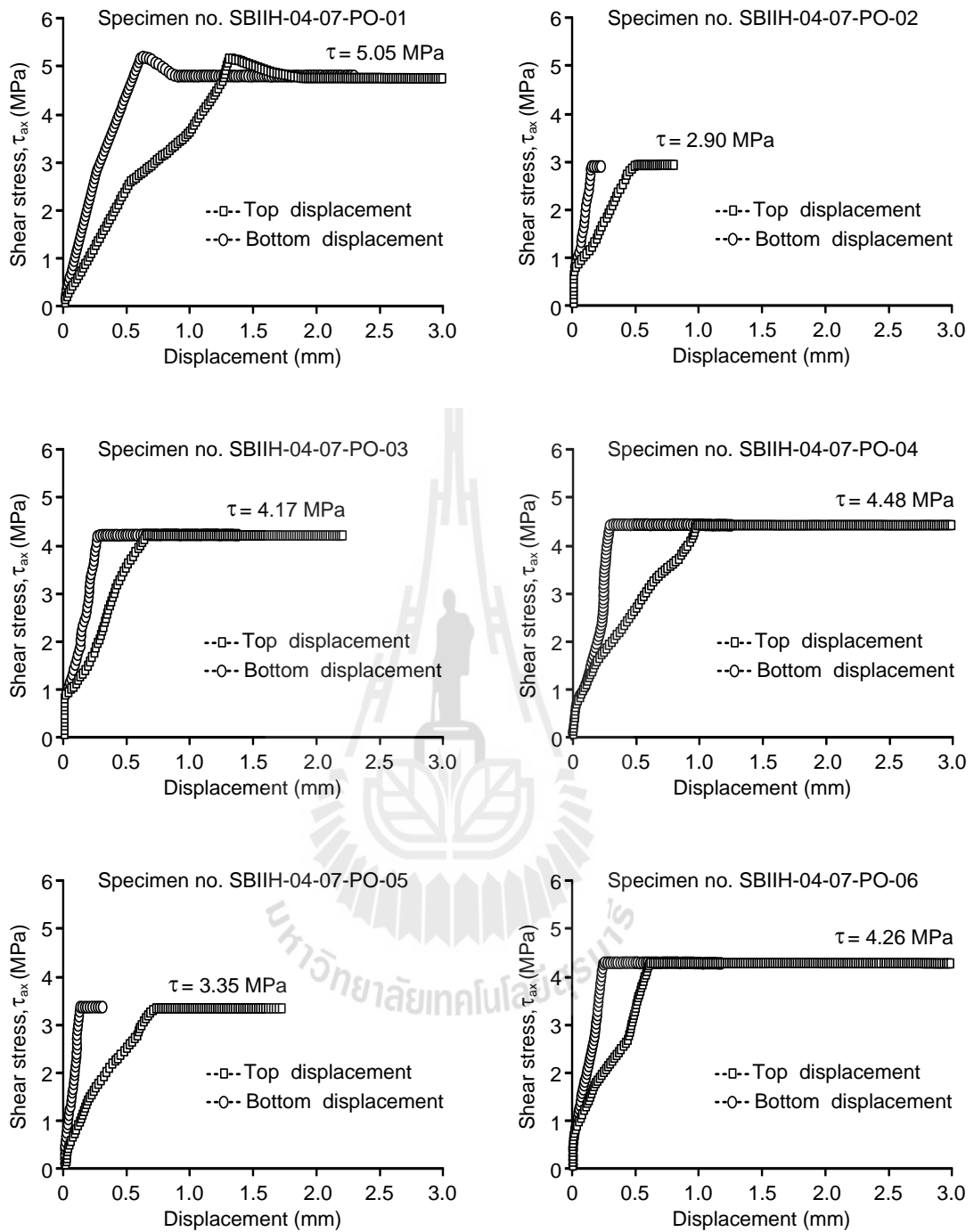


Figure 4.8 Applied shear stress as a function of the top and the bottom axial cement plug displacements for push-out tests.

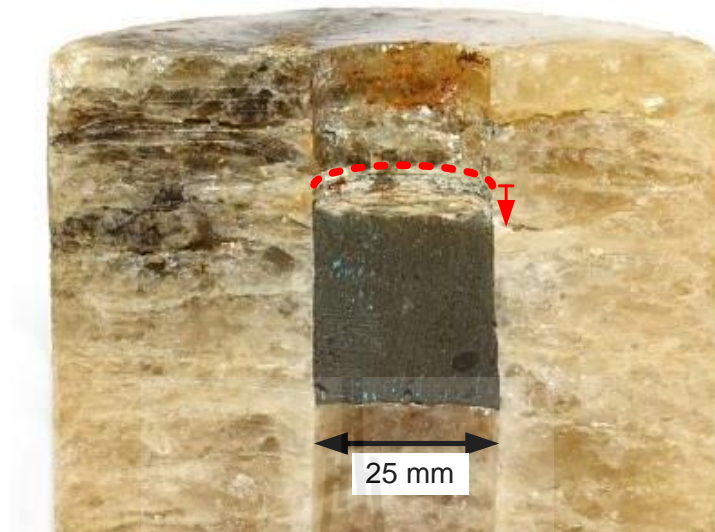


Figure 4.9 A cut section of specimen no. SBIIIH-04-07-PO-01 after failure in the push-out test.

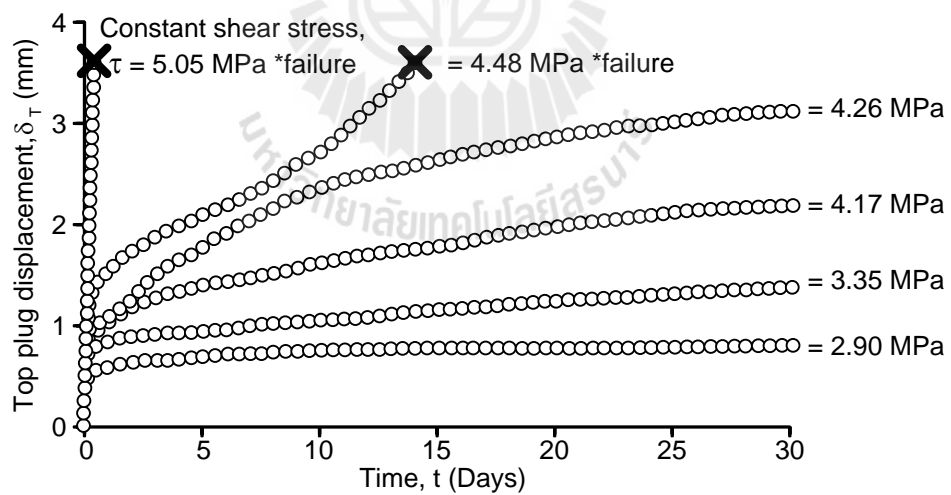


Figure 4.10 Top plug displacement (δ_T) as a function of time for push-out tests.

Table 4.7 Summary of the push-out tests.

Specimen type	D _o (mm)	L (mm)	D _i (mm)	L _h (mm)	L _c (mm)	F (kN)	P (kN)	σ _{ax} (MPa)	σ (MPa)	τ _{ax} (MPa)	τ (MPa)
SBIH-04-07-PO-01	98.42	100.39	25.81	20.90	28.71	11.77	-	22.48	-	5.05	-
SBIH-04-07-PO-02	100.21	100.53	25.68	18.86	32.67	-	7.64	-	14.74	-	2.90
SBIH-04-07-PO-03	100.01	104.02	25.22	22.02	28.90	-	9.55	-	19.11	-	4.17
SBIH-04-07-PO-04	100.18	101.27	25.63	19.50	29.11	-	10.50	-	20.35	-	4.48
SBIH-04-07-PO-05	100.25	100.07	26.35	19.50	30.17	-	8.37	-	15.34	-	3.35
SBIH-04-07-PO-06	101.23	102.33	26.23	19.78	28.55	-	10.02	-	18.55	-	4.26

D_o = Rock Salt Diameter, L = Rock Salt Length, D_i = Hole Diameter, L_h = Top Hole Length, L_c = Cement Plug Length,

F = Axial Load at Failure, P = Applied Constant Load, σ_{ax} = Axial Stress at Failure, σ = Constant Axial Stress, τ_{ax} = Shear Strength,

τ = Constant Shear Stress

4.4 Direct shear test

The shearing resistance between cement grout and rock salt fracture is determined by the direct shear testing. The test procedure is similar to the ASTM D5607 standard practice. The cement slurry is casted on 100 mm diameter saw cut fracture surfaces. The cement is cured for 7 days prior to testing for all tests. The direct shear machine model EL-77-1030 with both of the maximum shear load and normal load of 50 kN is used. Laboratory arrangement for the direct shear test equipment is shown in Figure 4.11. Pre-defined normal loads are maintained constant by during test. The constant normal stresses are 0.62, 1.26, 1.89, 2.52 and 3.14 MPa. Shear force is continuously applied and monitored for every 0.2 mm of the shear displacement.

The peak and the residual shear stress are calculated and plotted against the corresponding normal stress. Linear relationship between shear and normal stresses is obtained. According to the Coulomb criterion the peak and the residual friction angles at the cement-rock salt interface are 44 and 42 degrees, respectively. The cohesion of peak shear strength is 2.12 MPa, respectively (Figures 4.12 and 4.13).

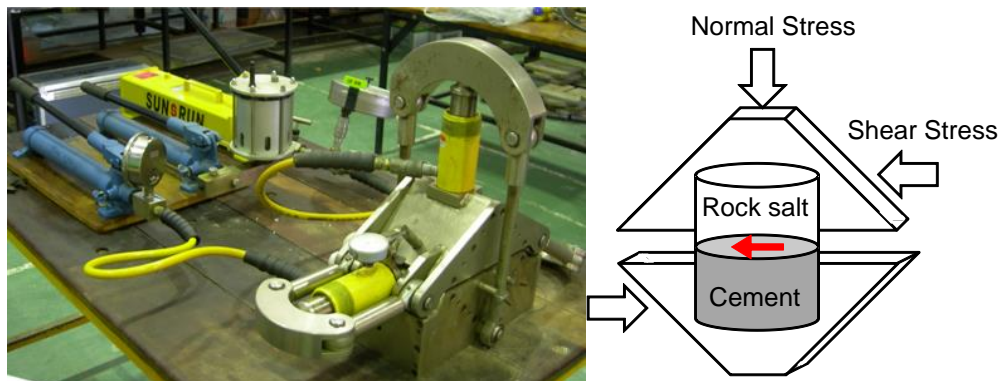


Figure 4.11 The direct shear machine model EL-77-1030 for direct shear tests.

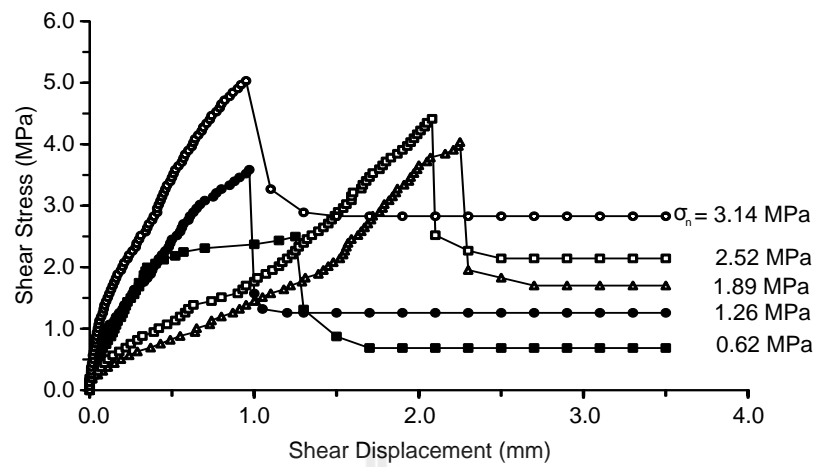


Figure 4.12 Shear stress as a function of shear displacement for SBIIH specimens.

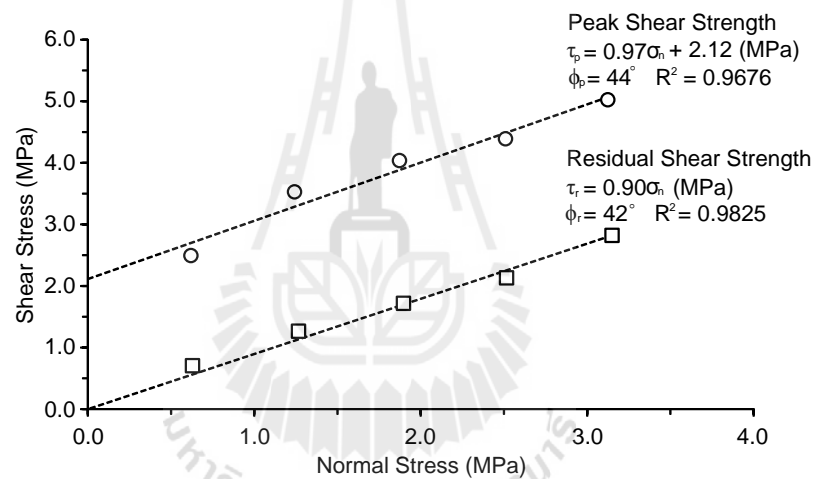


Figure 4.13 Shear stress as a function of normal stress for SBIIH specimens.

Table 4.8 Summary of shear strength parameters calibrated from direct shear tests using Coulomb's criteria.

Specimen type	σ_n (MPa)	τ_p (MPa)	c_p (MPa)	ϕ_p (degrees)	τ_r (MPa)	ϕ_r (degrees)
SBIIH-04-07-DS-01	0.62	2.50	2.12	44	0.69	42
SBIIH-04-07-DS-02	1.26	3.52			1.26	
SBIIH-04-07-DS-03	1.89	4.03			1.70	
SBIIH-04-07-DS-04	2.52	4.41			2.14	
SBIIH-04-07-DS-05	3.14	5.03			2.83	

The long-term direct shear tests of the cement-rock salt interface with a series of relatively long curing time with a constant normal stress and constant shear stress using a direct shear machine model DR-44 (Figure 4.14) the constant normal stress and constant shear stress for long-term testing, the average normal stiffness (k_n) and average shear stiffness (k_s) are 8.42 ± 3.00 GPa/m and 9.86 ± 2.93 GPa/m are shown in Table 4.9. The shear displacement is a function of both the normal stress and the shear stress of the fracture. Under a constant normal stress, the shear displacement (or creep deformation) is expected to increase as the shear stress is increased. Figure 4.15 show shear displacement as a function of time with a constant normal stress of 1.86 MPa.



Figure 4.14 The direct shear machine model DR-44 for long-term direct shear tests.

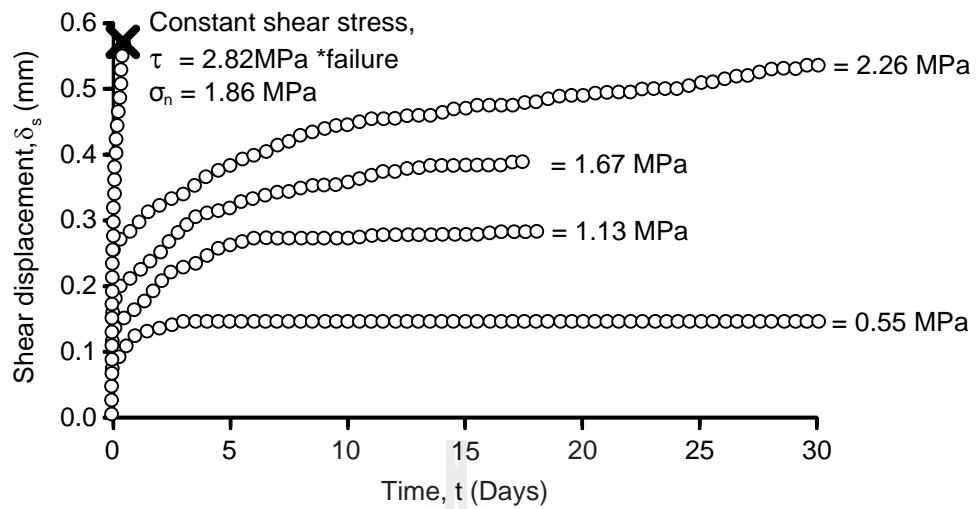


Figure 4.15 Shear displacements (δ_s) as a function of time for long-term direct shear tests with a constant normal stress of 1.86 MPa.

Table 4.9 Constant normal stress and constant shear stress for long-term direct shear tests.

Specimen type	Constant normal stress, σ_n (MPa)	Constant shear stress, τ (MPa)	k_n (GPa/m)	k_s (GPa/m)
SBIH-04-07-DS-06	1.86	1.13	7.67	6.60
SBIH-04-07-DS-07		1.67	12.24	11.25
SBIH-04-07-DS-08		2.26	10.27	12.17
SBIH-04-07-DS-09		2.82	7.61	6.77
SBIH-04-07-DS-10		0.55	4.33	12.50
Average			8.42±3.00	9.86±2.93

4.5 Permeability tests of cement grout

The permeability of grouting materials is determined in term of the intrinsic permeability (k). The constant head flow test is conducted to measure the longitudinal permeability of the grout. Test pressure and specimen configuration are measured and used to calculate the coefficient of permeability. The permeability of a system considered herein is measured using a constant head apparatus as shown on Figure 4.16. The flow in longitudinal direction of a tested system is described by Darcy's law. The coefficient of permeability (K) can be calculated from the equation (Indraratna & Ranjith, 2001).

$$K = Q / Ai \quad (4.2)$$

Where Q is volume flow rate (m^3/s), A is cross-sectional area of cement grout (m^2) and i is the hydraulic gradient. The intrinsic permeability (k) can be determined from the equation.

$$k = K\mu / \gamma \quad (4.3)$$

Where K is the coefficient of permeability (m/s), μ is dynamic viscosity of brine and γ is density of brine.

The cylinder specimen is 100 mm in diameter and 100 mm long. After one days of curing, the specimen is carefully removed from the cast (PVC pipe), cleaned, and placed in a brine bath before installing in the permeability test apparatus. The permeability of the test system is measured and recorded at 1, 3, 7, 14, 21, 28, 35, 42,

60, 109, 136 and 254 days of curing periods.

The coefficient of permeability (K) and intrinsic permeability (k) of cement grouts as a function of curing time is shown in Figures 4.17 and 4.18. Table 4.10 summarize the results of permeability testing. The results indicate that when the curing time increases the intrinsic permeability of cement grout decreases.

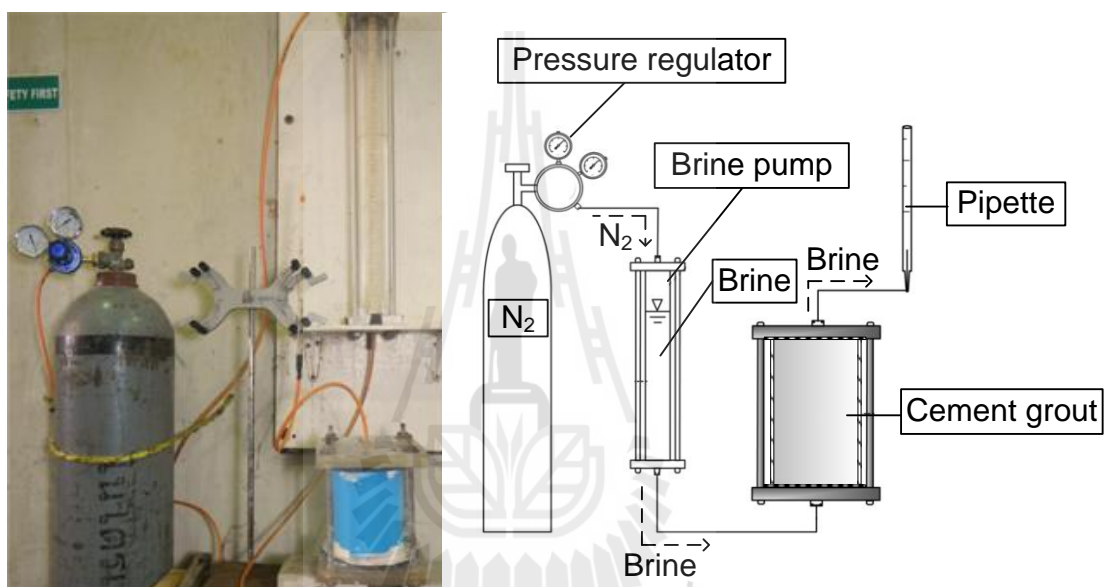


Figure 4.16 Constant head flow test apparatus used for the permeability testing of a cement grout.

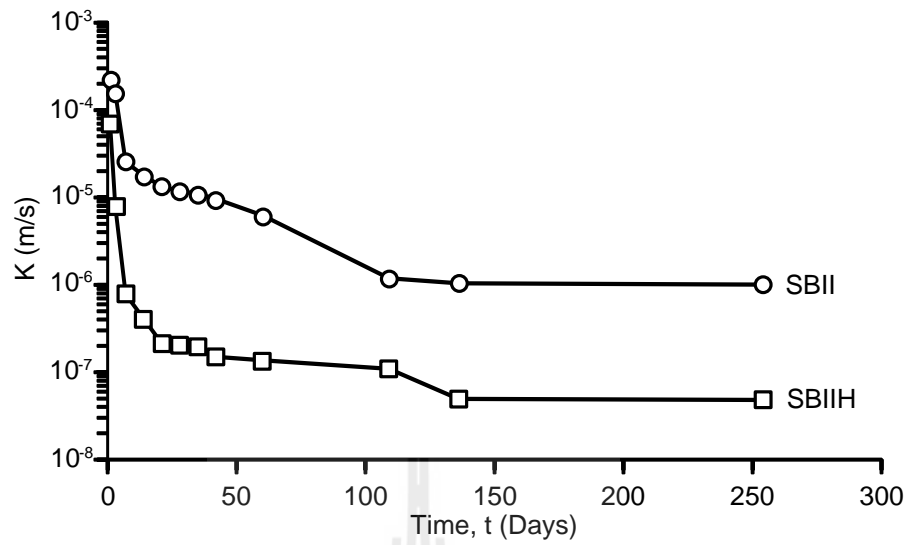


Figure 4.17 Coefficient of permeability (K) of the cement grouts.

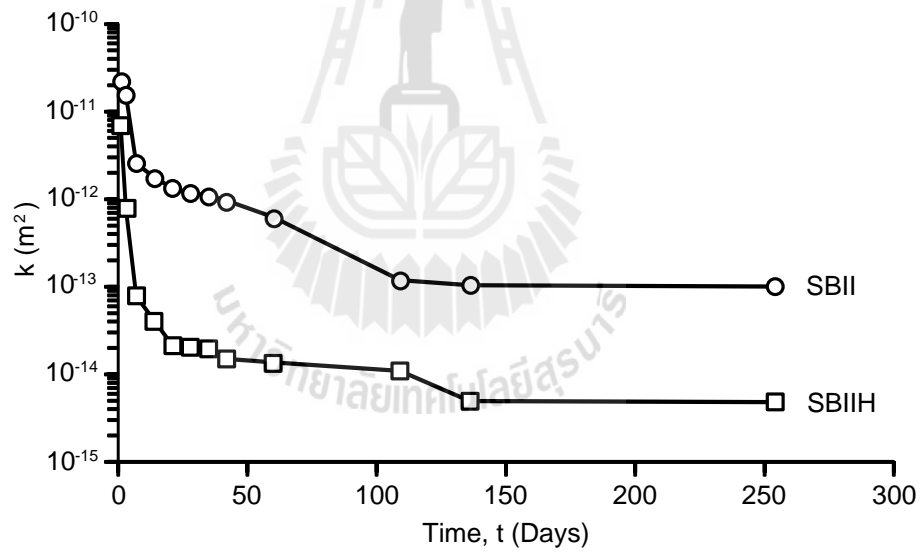


Figure 4.18 Intrinsic permeability (k) of the cement grouts.

Table 4.10 Summary of permeability testing of grouting.

Curing time (days)	Coefficient of permeability, K (m/s)		Intrinsic permeability, k (m ²)	
	SBII	SBIH	SBII	SBIH
1	2.10x10 ⁻⁴	6.91x10 ⁻⁵	2.15x10 ⁻¹¹	7.10x10 ⁻¹²
3	1.57x10 ⁻⁴	7.86x10 ⁻⁶	1.61x10 ⁻¹¹	8.06x10 ⁻¹³
7	2.54x10 ⁻⁵	7.83x10 ⁻⁷	2.61x10 ⁻¹²	8.04x10 ⁻¹⁴
14	1.79x10 ⁻⁵	4.09x10 ⁻⁷	1.84x10 ⁻¹²	4.20x10 ⁻¹⁴
21	1.33x10 ⁻⁵	2.15x10 ⁻⁷	1.37x10 ⁻¹²	2.20x10 ⁻¹⁴
28	1.18x10 ⁻⁵	2.09x10 ⁻⁷	1.21x10 ⁻¹²	2.15x10 ⁻¹⁴
35	1.10x10 ⁻⁵	2.01x10 ⁻⁷	1.13x10 ⁻¹²	2.06x10 ⁻¹⁴
42	9.67x10 ⁻⁶	1.50x10 ⁻⁷	9.93x10 ⁻¹³	1.54x10 ⁻¹⁴
60	6.22x10 ⁻⁶	1.37x10 ⁻⁷	6.39x10 ⁻¹³	1.40x10 ⁻¹⁴
109	1.19x10 ⁻⁶	1.09x10 ⁻⁷	1.22x10 ⁻¹³	1.12x10 ⁻¹⁴
136	1.04x10 ⁻⁶	4.95x10 ⁻⁸	1.07x10 ⁻¹³	5.08x10 ⁻¹⁵
254	1.00x10 ⁻⁶	4.81x10 ⁻⁸	1.03x10 ⁻¹³	4.94x10 ⁻¹⁵



CHAPTER V

CALIBRATION OF CREEP PARAMETERS

5.1 Objectives

The purpose of this chapter is to determine the calibration results of the displacement and transient shear creep parameters. The regression analysis of the proposed shear creep strain equation with the IBM SPSS Statistics 19 (Wendai, 2000) is performed to determine the elastic shear modulus, the visco-elastic shear modulus and visco-coefficient. The test results from laboratory measurements in term of the applied shear stress along borehole plug and the applied shearing resistant between cement grout and rock salt as a function of time.

5.2 Visco-elastic shear creep model

The visco-elastic shear creep behavior of the shear stress along borehole plug and the shearing resistant between cement grout and rock salt is approached by two components, The behavior of the elastic component (Hookean body) and the viscosity component (Newton body) and the two components can be connected in series (Maxwell model) and parallel (Kelvin models).

In the Kelvin models form visco-elastic model in combination with the elastic behavior of the viscous behavior connected parallel and series elastic behavior (Hookean). In this research, the Hookean-Kelvin model (Figure 5.1) is chosen to determine the visco-elastic shear creep behavior between bond cement and rock salt.

The creep equation of Hookean-Kelvin model under the action of the applied constant shear stress (τ) is;

$$\delta = \frac{\tau}{G_1} + \frac{\tau}{G_2} \left[1 - \exp\left(-\frac{G_2 t}{\eta_1}\right) \right] \quad (5.1)$$

where δ is the shear displacements, t is time, G_1 is the elastic shear modulus, G_2 is the visco-elastic shear modulus and η_1 is the viscous coefficient (Yang and Cheng, 2011; Saptono et al., 2012).

The creep parameters for Hookean-Kelvin model can be determined by following method. The elastic shear modulus G_1 is obtained by $G_1 = \tau/\delta_0$, where δ_0 is the instantaneous shear displacement for each constant shear stress. After confirming the parameter G_1 , the creep parameters G_2 and η_1 can be obtained by the regression analysis using SPSS program. When identifying, one of the correlation coefficient (R^2) is regarded as the discrimination criterion.

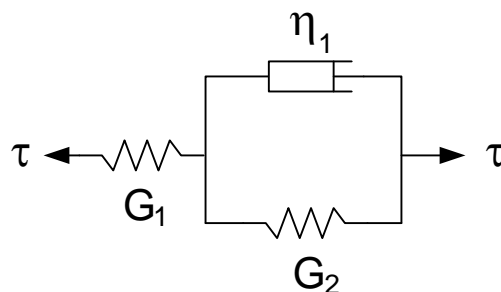


Figure 5.1 Hookean-Kelvin model (Yang and Cheng, 2011).

5.3 Creep parameters of push-out tests

The push-out tests are performed on cement plugs are plotted the top plug displacements (δ_T) as a function of time with a various constant shear stress for long-term. From the short-term push-out test result, the axial shear strength (bond strength, τ_{av}) of borehole cement plug is 5.05 MPa. Therefore five applied constant shear stress (τ) levels, 0.29, 3.35, 4.17, 4.26 and 4.48 MPa, are used to investigate visco-elastic shear creep behavior between cement plug and rock salt. The relation between shear displacement and time are obtained with a various constant shear stress levels for 30 days.

The Figure 5.2 shows the obtained typical shear creep test results between cement plug and rock salt specimens with five various applied constant shear stress levels. The results indicate that top plug displacements expected to increase as the shear stress is increased, which can be represented by creep equation of Hookean-Kelvin model.

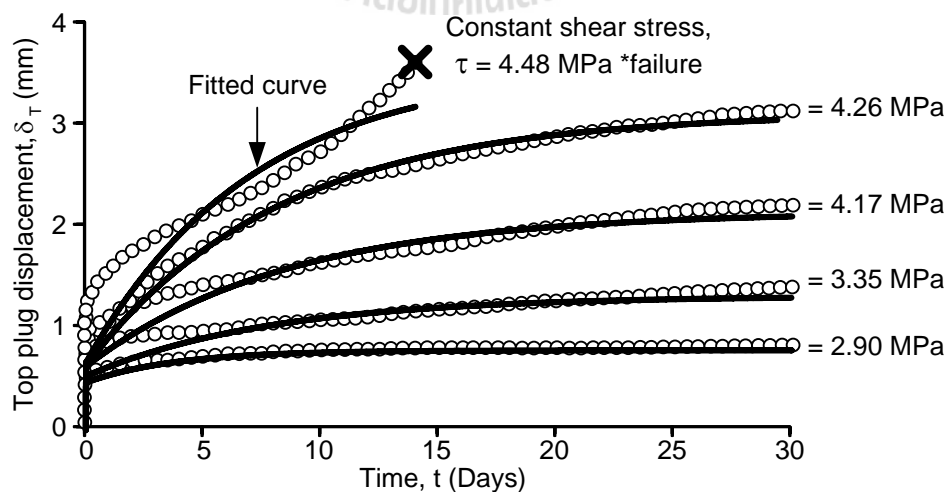


Figure 5.2 The push-out test results (points) and back predictions (lines).

In accordance with Figure 5.2 and Equation 5.1, the creep parameters for Hookean-Kelvin model can be identified by the following method in section 5.2. Determination of shear elastic modulus (G_1) is obtained from the ratio between applied constant shear stress and instantaneous shear displacement (τ/δ_0). After getting the parameter G_1 , further G_2 and η_1 determined by using SPSS Statistics software through the iteration of Equation 5.1. Table 5.1 lists the shear creep model parameters with five shear stress levels at time scale of 30 days. A maximum values of R^2 are obtained.

Table 5.1 Creep parameters calibrated from push-out test results.

$\delta_T = \frac{\tau}{G_1} + \frac{\tau}{G_2} \left[1 - \exp\left(-\frac{G_2}{\eta_1} t\right) \right] \text{ (mm)}$					
τ (MPa)	τ/τ_{av}	G_1 (MPa·mm ⁻¹)	G_2 (MPa·mm ⁻¹)	η_1 (MPa·Days·mm ⁻¹)	R^2
2.90	0.57	6.257	9.181	34.470	0.935
3.35	0.66	6.382	4.272	33.272	0.804
4.17	0.83	6.699	2.760	23.611	0.918
4.26	0.84	6.777	1.725	14.103	0.985
4.48	0.89	6.849	1.546	10.830	0.860
*t (Days)					

The fitting parameters of elastic shear modulus (G_1), visco-elastic shear modulus (G_2) and viscous coefficient (η_1) are plotted as function of the applied constant shear ratio (τ/τ_{av}), where τ is the applied constant shear and τ_{av} is the axial shear strength (bond strength) of borehole cement plug, as shown in Figure 5.3. The empirical parameters, G_1 increase slightly with the τ/τ_{av} increase. The parameters of G_2 and η_1 tend to decrease in term of increasing applied constant shear ratio with a power relation. By adopting the parameter and relation with the applied constant

shear stress listed in Table 5.1, the set of equations in Table 5.2 can be used to predict the visco-elastic behavior for any shear stress levels.

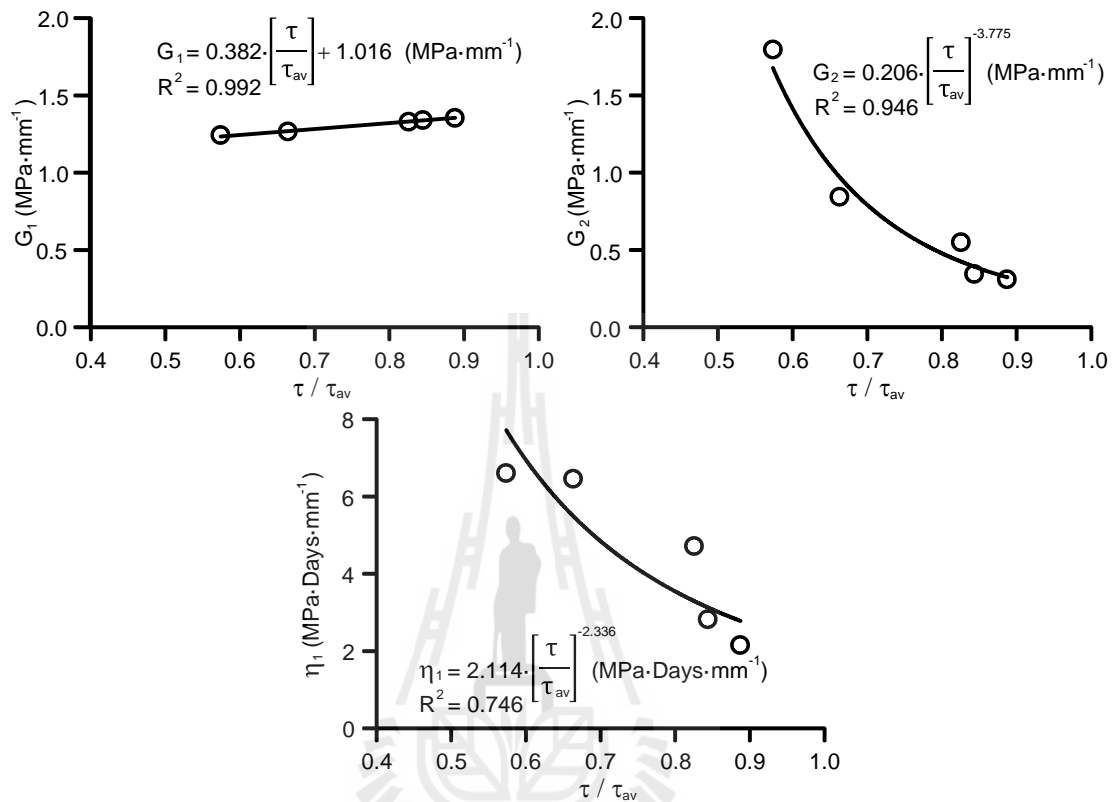


Figure 5.3 Influence of applied stress ratio (τ/τ_{av}) on the elastic shear modulus (G_1), visco-elastic shear modulus (G_2) and viscous coefficient (η_1).

Table 5.2 The empirical parameters of elastic shear modulus, visco-elastic shear modulus and viscous coefficient with applied stress ratio.

Empirical equations	Empirical parameters		
	χ	κ	R^2
$G_1 = \chi \cdot \left[\frac{\tau}{\tau_{av}} \right] + \kappa$ (MPa·mm ⁻¹)	0.382	1.016	0.992
$G_2 = \alpha \cdot \left[\frac{\tau}{\tau_{av}} \right]^\beta$ (MPa·mm ⁻¹)	α	β	R^2
	0.206	-3.775	0.946
$\eta_1 = \lambda \cdot \left[\frac{\tau}{\tau_{av}} \right]^\omega$ (MPa·Days·mm ⁻¹)	λ	ω	R^2
	2.114	-2.336	0.746

5.4 Creep parameters of long-term direct shear tests

The long-term direct shear tests of the cement-rock salt interface are plotted the shear displacement (δ_s) as a function of time with a various constant shear stress. The constant normal stress is set to 1.86 MPa, and the corresponding peak shear strength (τ_p) is 3.92 MPa in accordance with direct shear equation in Chapter IV. Therefore four stress levels, 0.55, 1.13, 1.67 and 2.26 MPa, are used to determine visco-elastic shear creep behavior of the cement-salt interface, and then applied the corresponding shear stress level. The relation between shear displacement and time are obtained as function of time with 30 days.

Figure 5.4 shows the plotted typical shear creep test results of specimen with four various shear stress levels. The results indicate that the cement-salt interface exists instant deformation at constant normal stress. With the long-term, the shear deformation of specimen also increase step by step, but shear rate decreases gradually.

Table 5.3 shows the shear creep model parameters of long-term direct shear tests. The ratio of constant shear stress (τ) to peak shear strength (τ_p) which is called the shear stress ratio (τ/τ_p). The fitting parameters of elastic shear modulus (G_1), visco-elastic shear modulus (G_2) and viscous coefficient (η_1) with shear stress ratio (τ/τ_p). The empirical parameters are elastic shear modulus, visco-elastic shear modulus and viscous coefficient change with the increase in the shear stress ratio, the increasing shear stress ratio will increase elastic shear modulus, visco-elastic shear modulus and viscous coefficient (Figure 5.5). Table 5.4 show the set of equations that can be used to predict the visco-elastic behavior for any shear stress levels.

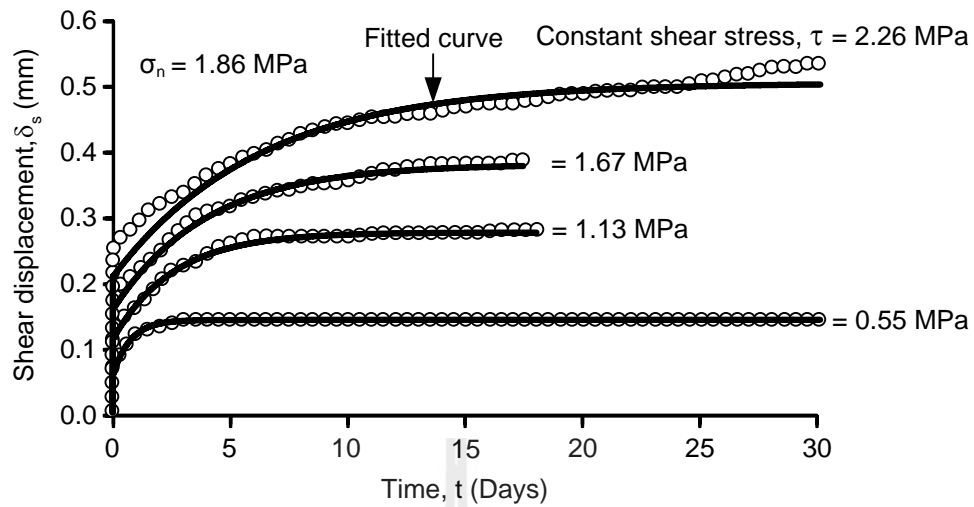


Figure 5.4 The long-term direct shear test results (points) and back predictions (lines).

Table 5.3 Creep parameters calibrated from long-term direct shear test results.

$\delta_s = \frac{\tau}{G_1} + \frac{\tau}{G_2} \left[1 - \exp\left(-\frac{G_2}{\eta_1} t\right) \right] \text{ (mm)}$					
τ (MPa)	τ / τ_p	G_1 (MPa·mm ⁻¹)	G_2 (MPa·mm ⁻¹)	η_1 (MPa·Days·mm ⁻¹)	R^2
0.55	0.14	10.061	6.510	4.792	0.991
1.13	0.29	10.237	6.924	17.735	0.982
1.67	0.43	10.804	7.572	30.052	0.986
2.26	0.58	11.029	7.681	47.361	0.955
*Constant normal stress, $\sigma_n = 1.86$ MPa					
*t (Days)					

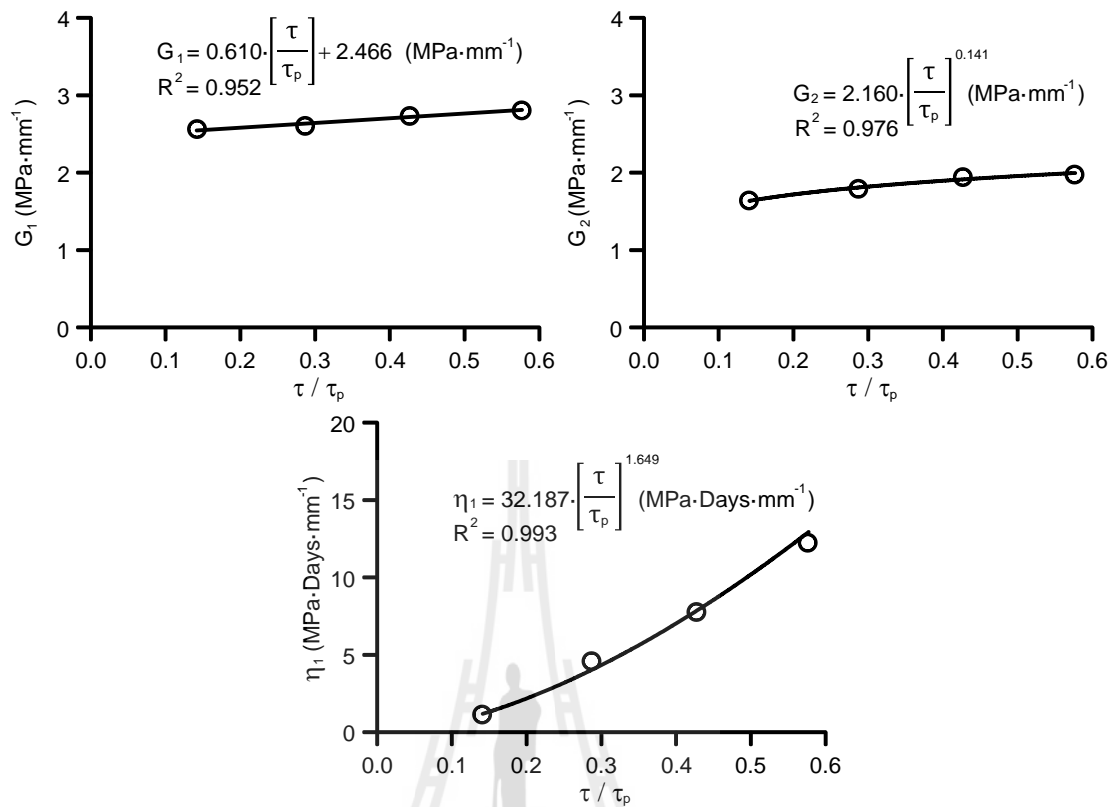


Figure 5.5 Influence of shear stress ratio (τ/τ_p) on the elastic shear modulus (G_1), visco-elastic shear modulus (G_2) and viscous coefficient (η_1).

Table 5.4 The empirical parameters of elastic shear modulus, visco-elastic shear modulus and viscous coefficient with shear stress ratio.

Empirical equations	Empirical parameters		
	χ	κ	R^2
$G_1 = \chi \cdot \left[\frac{\tau}{\tau_p} \right] + \kappa$ (MPa·mm ⁻¹)	0.382	1.016	0.992
$G_2 = \alpha \cdot \left[\frac{\tau}{\tau_p} \right]^\beta$ (MPa·mm ⁻¹)	α	β	R^2
	0.206	-3.775	0.946
$\eta_1 = \lambda \cdot \left[\frac{\tau}{\tau_p} \right]^\omega$ (MPa·Days·mm ⁻¹)	λ	ω	R^2
	2.114	-2.336	0.746

CHAPTER VI

DISCUSSIONS, CONCLUSIONS AND RECOMMENDATIONS FOR FUTURE STUDIES

6.1 Discussions and conclusions

The long-term of frictional shear strengths of cement sealing in rock salt have been experimentally determined by series of borehole push-out testing and direct shear testing. The results are used to assist in design of the cement seals in the rock salt to minimize brine circulation and potential leakage along a main access of salt mine at the long time. The salt specimens are prepared from 100 mm diameter cores drilled from Middle member of the Maha Sarakham formation. The cement seal is prepared from commercial grade Portland-pozzolan cement, saturated brine, anti-form agent and liquid additive. The two types of cement used are the Salt-bond II with low brine content (SBII) cement and the Salt-bond II with high brine content (SBIIIH) cement. The cement grouts are prepared to determine the mechanical and hydraulic performance of cement sealing in rock salt. This study aim to determine the appropriate are minimum slurry viscosity and minimum permeability of the mixed cement grouting. In order to obtain sufficient mechanical and hydraulic performance of borehole sealing, SBIIIH cement is recommended.

Characterization test results of the high brine content (SBIIIH) cement indicate that when the curing time increases the uniaxial compressive strength, the elastic modulus, and the Brazilian tensile strength of cement grout increases. The uniaxial

compressive, the elastic modulus and Brazilian tensile strengths after 60 days curing times are 20.34 ± 3.42 MPa, 1.87 ± 0.38 GPa and 2.75 ± 0.18 MPa, respectively. The average dynamics and kinematic viscosity of cement slurry are 4.53 Pa·s and 2.59×10^{-3} m²/s, respectively. The average cement slurry density is 1.75 g/cc.

The long-term permeability of the cement grouting materials measured from the longitudinal flow test with constant head decreases with curing time at 1, 3, 7, 14, 21, 28, 35, 42, 60, 109, 136 and 254 days. The results indicate that when the curing time increases the coefficient of permeability (K) and the intrinsic permeability (k) of the cement grout decreases. The coefficient of permeability and the intrinsic permeability after 254 days curing times are 4.81×10^{-8} m²/s and 4.95×10^{-15} m², respectively.

The push-out tests and the direct shear tests are performed to determine the bond strength of cement plugs in rock salt. The cement slurry is casted in the 25 mm diameter borehole with a length of 30 mm for the push-out testing and on 100 mm diameter fracture saw cut surface for the direct shear testing. For all tests the cement is cured for 7 days prior to testing.

The short-term direct shear tests results indicate the frictional resistance at cement-salt interface with the friction angle of 44 degrees and cohesion of 2.12 MPa. The average normal stiffness is 8.42 ± 3.00 GPa/m. The average shear stiffness is 9.86 ± 2.93 GPa/m. The short-term push-out test results show significantly higher frictional resistance at the interface than does the direct shear testing. The axial shear strength of the borehole cement seal is 5.05 MPa. This is primarily due to the effect of the Poisson's ratio which increases the normal (radial) stress at the cement-salt interface while the axial load is applied. This implies that the direct shear test results

may give an overly conservative estimate of the shearing resistance between the rock salt and cement seal.

The long-term push out tests are performed on cement plugs with a series of relatively long curing time with the constant shear stress. The results plot the top plug displacements as a function of time with a various constant shear stress and show an instantaneous elastic strain. Base on the visco-elastic shear creep behavior results of the bond cement-rock salt interface with a various shear stress levels. Therefore five applied constant shear stress levels, 0.29, 3.35, 4.17, 4.26 and 4.48 MPa, are used to investigate visco-elastic shear creep behavior between cement plug and rock salt. The relation between shear displacement and time are obtained with a various constant shear stress levels for 30 days.

The Hookean-Kelvin models is chosen to determine the visco-elastic shear creep behavior between bond cement and rock salt coefficient (Yang and Cheng, 2011; Saptono et al., 2012). The fitting parameters of elastic shear modulus (G_1), visco-elastic shear modulus (G_2) and viscous coefficient (η_1) are plotted as function of the applied constant shear ratio (τ/τ_{av}) of borehole cement plug. The empirical parameters, G_1 increase slightly with the τ/τ_{av} increase. The parameters of G_2 and η_1 tend to decrease in term of increasing applied constant shear ratio with a power relation.

The long-term direct shear testing at a constant normal stress shows the creep displacement. Under a constant normal stress, the creep deformation is expected to increase as the shear is increased. The constant normal stress is set to 1.86 MPa. Therefore four stress levels, 0.55, 1.13, 1.67 and 2.26 MPa. The relation between shear displacement and time are obtained as function of time with 30 days.

The long-term direct shear test results show the shear creep model parameters of long-term direct shear tests. The fitting parameters of elastic shear modulus (G_1), visco-elastic shear modulus (G_2) and viscous coefficient (η_1) with shear stress ratio (τ/τ_p). The empirical parameters are elastic shear modulus, visco-elastic shear modulus and viscous coefficient change with the increase in the shear stress ratio, the increasing shear stress ratio will increase G_1 , G_2 and η_1 . The predicted curve agree well with the experiment data, which shows the reasonability of nonlinear visco-elastic shear creep model.

6.2 Recommendations for future studies

The uncertainties of the studied investigation and results discussed above lead to the recommendations for further studies. More testing is required on a variety type of rock salt with different components of cement. Testing time and curing time should be longer (months or years) for long-term testing.

REFERENCES

- Akgun, H. (1996). Strength parameters of cement borehole seals in rock. **Sealing of Boreholes and Underground Excavations in Rock**. Chapman & Hall, London pp. 28–39.
- Akgun, H. (1997). An assessment of borehole sealing in a salt environment. *Environmental Geology* 31: 34-41.
- Akgun, H. and Daemen, J.J.K. (1997). Analytical and experimental assessment of mechanical borehole sealing performance in rock. **Engineering Geology** 47(3): 233-241.
- Akgun, H. and Daemen, J.J.K. (2002). Influence of degree of saturation on the borehole sealing performance of an expansive cement grout. **Cement and Concrete Research** 30(2): 281-289.
- Akgun, H. and Daemen, J.J.K. (2004). Stability of expansive cement grout borehole seals emplaced in the vicinity of underground radioactive waste repositories. **Environmental Geology** 45:1167-1171.
- Amadei, B., and Curran, J.H. (1982). Creep behaviour of rock joints. In: **Underground rock engineering: 13th Canadian Rock Mechanics Symposium**. Transactions of the Canadian Institute of Mining and Metallurgy, 22, pp. 146–150.
- American Petroleum Institute. (1986). Specifications for Materials and Testing for Well Cements. **3rd Edition American Petroleum Institute**, Production Department, Dallas, TX.
- ASTM C39-10. Standard Test Method for Compressive Strength of Cylindrical

- Concrete Specimens. **Annual Book of ASTM Standards** (Vol. 04.01). Philadelphia: American Society for Testing and Materials.
- ASTM C938-10. Standard Practice for Proportioning Grout Mixtures for Preplaced-Aggregate Concrete. In **Annual Book of ASTM Standards** (Vol. 04.02). Philadelphia: American Society for Testing and Materials.
- ASTM D2196-10. Standard Test Methods for Rheological Properties of Non-Newtonian Materials by Rotational (Brookfield type) Viscometer. **Annual Book of ASTM Standards** (Vol. 06.01). Philadelphia: American Society for Testing and Materials.
- ASTM D3967-08. Standard test Method for Splitting Tensile Strength of Intact Rock Core Specimens. **Annual Book of ASTM Standards** (Vol. 04.08). Philadelphia: American Society for Testing and Materials.
- ASTM D4543-85. Standard Test Method for Preparing Rock Core Specimens and Determining Dimensional and Shape Tolerances. **Annual Book of ASTM Standard**. Philadelphia: American Society for Testing and Materials.
- ASTM D5607-08. Standard Test Method for Performing Laboratory Direct Shear Strength Tests of Rock Specimens Under Constant Normal Force. **Annual Book of ASTM Standards** (Vol. 04.08). Philadelphia: American Society for Testing and Materials.
- ASTM D7012-10. Standard test Method for Compressive Strength and Elastic Moduli of Intact Rock Core Specimens under Varying States of Stress and Temperatures. **Annual Book of ASTM Standards** (Vol. 04.09). Philadelphia: American Society for Testing and Materials.
- ASTM D854-10. Standard Test Methods for Specific Gravity of Soil Solids by Water

- Pycnometer. **Annual Book of ASTM Standards** (Vol. 04.08). Philadelphia: American Society for Testing and Materials.
- Boa, J.A., Jr., (1978). Borehole Plugging Program (Waste Disposal): Initial Investigations and Preliminary Data. Miscellaneous Paper C-78-1, Report 1, SAND 77-7005, prepared by **U.S. Army Laboratories**, Albuquerque, NM.
- Brodsky, N. S., F. D. Hansen, and T. W. Pfeifle. (1998). Properties of dynamically compacted WIPP Salt. In **Proceedings of the Fourth Conference on the Mechanical Behavior of Salt** (pp. 303-316), Clausthal-Zellerfeld, Germany, Trans Tech Publications.
- Brown, E.T. (editor). (1981). Rock Characterization testing and Monitoring: ISRM Suggested methods. The Commission on Rock Testing Methods, **International Society for Rock Mechanics**, Pergamon Press, Now York, pp. 211.
- Daemen, J.J.K. and Fuenkajorn, K. (1996). Design of Boreholes Seals-Processes, Criteria and Considerations. **Sealing of Boreholes and Underground Excavations in Rock**, Chapman & Hall, London, pp. 267-279.
- Dale, T. and Hurtodo, L, D. (1998). WIPP air-intake shaft disturbed-rock zone study. In **Proceedings of the Fourth Conference on the Mechanical Behavior of Salt** (pp. 525-535), Clausthal-Zellerfeld, Germany, Trans Tech Publications.
- Dieterich, J.H. (1972). Time-dependent friction in rocks. **Journal of Geophysical Research**, 77, pp. 3690–3697.
- Dusseault, M.B. and Fordham, C.J. (1993). Time-dependent behavior of rocks. Comprehensive Rock Engineering Principles, Practice and Project: **Rock Testing and Site Characterization** (Vol. 3, pp. 119-149). London,

Pergamon.

- Econoides, M.J., Watters, L.T. and Dunn-Norman, S. (1998). **Petroleum well construction**. Chichester: John Wiley & Sons.
- Fuenkajorn, K. and Daemen, J.J.K. (1987). Mechanical Interaction between Rock and Multi-component Shaft or Borehole Plugs. **Rock Mechanics: Proceedings of the 28th U.S. Symposium**, June 29-July 1, University of Arizona, Tucson, pp. 165-172.
- Fuenkajorn, K. and Daemen, J.J.K. (1988). Borehole Closure in Salt. **Key Questions in Rock Mechanics: Proceedings of the 29th U.S. Symposium**, June 13-15, University of Minnesota, Minneapolis, pp. 191-198.
- Fuenkajorn, K. and Daemen, J.J.K. (1996). Design Guideline for Mine Sealing. **The 1996 Arizona Conference**, Tucson, Arizona, December 8-9.
- Fuenkajorn, K. and Daemen, J.J.K. (1996). Sealing of Boreholes in Rock-An Overview. **2nd North American Rock Mechanics**, Symposium, Montreal, Quebec, Canada, pp. 1447-1454.
- Fuenkajorn, K. and Phueakphum, D. (2010). Effects of cyclic loading on mechanical properties of Maha Sarakham salt. **Engineering Geology** 112: 43-52.
- Gray, T.A. and Gray, R.E. (1992). Mine closure, sealing, and abandonment. **SME mining handbook**. 1, 2: 659-674.
- Gulick, C.W., Jr., J.A. Boa, Jr., and A.D. Buck, 1980. Bell Canyon Test (BCT) Cement Grout Development Report. SAND 80-1928, **Sandia National Laboratories**, Albuquerque, NM.
- Indraratna, B. and Ranjith, P. (2001). **Hydromechanical Aspects and Unsaturated Flow in Joints Rock**. Lisse: A. A. Balkema.

- Jeremic, M. L. (1994). **Rock mechanics in salt mining** (530 pp.). Rotherdam: A. A. Balkema.
- Knowles, M. K., Borns, D., Fredrich, J., Holcomb, D., Price, R. and Zeuch, D. (1998). Testing the disturbed zone around a rigid inclusion in salt. In **Proceedings of the Fourth Conference on the Mechanical Behavior of Salt** (pp. 175-188). Clausthal, Germany: Trans Tech Publications.
- Lajtai, E.Z., and Gadi, A.M. (1989). Friction on a granite to granite interface. **Rock Mechanics and Rock Engineering**, 22, pp 25–49.
- Ouyang, S., and Daemen, J.J.K. (1996). Performance of bentonite and bentonite/crushed rock borehole seals. **Sealing of Boreholes and Underground Excavations in Rock**, Chapman & Hall, London pp. 65-95.
- Peach, C.J. (1991). Influence of deformation on the fluid transport properties of salt rock. **Geological Ultraiectina** No. 77, Netherlands.
- Ran, C., Daemen, J.J.K., Schuhen, M.D. and Hansen, F.D. (1997). Dynamic compaction properties of bentonite. **International Journal of Rock Mechanics and Mining Sciences** 34(1-4).
- Roy, D.M., M.W. Grutzeck and L.D. Wakeley, (1983). Selection and Durability of Seal Materials for a Bedded Salt Repository: Preliminary Studies, ONWI-479. Prepared by the **Materials Research Laboratory**, The Pennsylvania State University, and Structures Laboratory, U.S. Army Engineer Waterways Experiment Station, for the office of Nuclear Waste Isolation, Battelle Memorial Institute, Columbus, OH.
- Roy, D.M., M.W. Grutzeck and L.D. Wakeley, (1985). Salt Repository Seal Materials: A Synopsis of Early Cementitious Materials Development,

- BMI/ONWI-536. Prepared by the **Materials Research Laboratory**, The Pennsylvania State University, and Structures Laboratory, U.S. Army Engineer Waterways Experiment Station, for the office of Nuclear Waste Isolation, Battelle Memorial Institute, Columbus, OH.
- Roy, D.M., M.W. Grutzeck, K. Mather, and A.D. Buck, (1982). PSU/WES Interlaboratory Study of an Experimental Cementitious Repository Seal Material, ONWI-324. Prepared by the **Materials Research Laboratory**, The Pennsylvania State University, and Structures Laboratory, U.S. Army Engineer Waterways Experiment Station, for the office of Nuclear Waste Isolation, Battelle Memorial Institute, Columbus, OH.
- Samaiklang, W. and Fuenkajorn, K. (2013). Mechanical and hydraulic performance of cement grouts from 5 suppliers in Thailand. **Rock Mechanics, Fuenkajorn & Phien-wej (eds)**, pp. 333-342.
- Samsri, P., Sriapai, T., Walsri, C. and Fuenkajorn, K. (2010). Polyaxial creep testing of rock salt. In **Proceedings of the Third Thailand Symposium on Rock**.
- Saptono, S., Kramadibrata, S., Sulistianto, B. and Priyadi (2012) Study on Long Term Strength Characteristic of Sandstone, Tutupan Coal Mine, South Kalimantan, Indonesia. **Proc. of 7th Asian Rock Mechanics Symposium**, Seoul, Korea, 15-19 October 2012, 1305-1310.
- Smith, D.K. (1993). **Handbook on Plugging and Abandonment**. Oklahoma: Penn Well Publishing Company.
- Smith, S.A. (1994). **Well & borehole sealing**. Ohio: Ground water publishing co.
- South, D.L. and Fuenkajorn, K. (1996). Laboratory Performance of Cement Boreholes Seals. **Sealing of Boreholes and Underground Excavations in**

- Rock**, Chapman & Hall, London, pp. 9-27.
- Stormont, J.C. (1990). Discontinuous behavior near excavations in a bedded salt formation. **Int. Jour. Mining and Geological Eng.** 8:35-36.
- Stormont, J.C. and Daemen, J.J.K. (1983). Axial Strength of Cement Borehole Plugs in Granite and Basalt. NUREG/CR-3594, **Topical Report on Rock Mass Sealing**, prepare for Division of Health, Siting and Waste Management, Office of Nuclear Regulatory Research, U.S. Nuclear Regulatory Commission, by the Department of Mining and Geological Engineering, University of Arizona, Tucson.
- Stormont, J.C. and Daemen, J.J.K. (1991). **Laboratory study of gas permeability changes in rock salt during deformation**. SAND90-2638 (p. 40), Sandia National Laboratories, Albuquerque, NM.
- Suwanich, P. (1986). Potash and Rock Salt in Thailand: Nonmetallic Minerals Bulletin No.2. **Economic Geology Division**, Department of Mineral Resources, Bangkok, Thailand.
- Tabakh, M.E., Utha-Aroon, C., Warren, J.K. and Schreiber, B.C. (2003). Origin of dolomites in the Cretaceous Maha Sarakham evaporates of the Khorat Plateau, northeast Thailand. **Sedimentary Geology**, 157: 235–252.
- Tepnarong, P. (2012). Bond strength of cement sealing in Maha Sarakham salt. **Proc. of 7th Asian Rock Mechanics Symposium**, Seoul, Korea, 15-19 October 2012, 584-593.
- Tepnarong, P. and Deethouw, P. (2014). Mechanical and Hydraulic Performance of Sludge-mixed Cement Borehole Plugs in Rock Salt. **Proc. of 8th Asian Rock Mechanics Symposium**, Sapporo, Japan, 14-16 October 2014.

- Utha-aroon, C. (1993). Continental origin of the Maha Sarakham evaporites, Northeastern Thailand. **Journal of Southeast Asian Earth Sciences**, 1993, Great Britain, Vol. 8(1-4), pp. 193-203.
- Wakeley, L.D. and D.M. Roy, (1985). Cementitious Mixtures for Sealing Evaporite and Clastic Rocks in a Radioactive-Waste Repository. Miscellaneous Paper SL-85-16, prepared by the Structures Laboratory, U.S. Army Engineer Waterways Experiment Station, and by the **Materials Research Laboratory**, The Pennsylvania State University, for the office of Nuclear Waste Isolation, Battelle Memorial Institute, Columbus, OH, and for Sandia National Laboratories, Albuquerque, NM.
- Wendai, L. (2000). Regression analysis, linear regression and probit regression in 13 chapters. **SPSS for Windows: statistical analysis**, Publishing House of Electronic Industry, Beijing.
- Wong, H.S., Zimmerman, R.W. and Buenfeld, N.R. (2011). Estimating the permeability of cement pastes and mortars using image analysis and effective medium theory. **Cement and Concrete Research** **42**, pp. 476-483.
- Yang, S.Q., Cheng, L. (2011) Non-Stationary and Nonlinear Visco-Elastic Shear Creep Model for Shale. **International Journal Rock Mechanics & Mining Sciences**, Volume 48, Issue 6, 1011-1020.

BIOGRAPHY

Mr. Sakeereen Pattani was born on May 18, 1989 in Narathiwat province, Thailand. He received his Bachelor's Degree in Engineering (Geotechnology) from Suranaree University of Technology in 2011. After graduation, he has employed under the position of Geotechnical Engineering by International Engineering Consultants Co., Ltd (IEC). Since 2013, he continued to study with a Master's degree in the Geological Engineering Program, Institute of Engineering, Suranaree University of Technology. During graduation in 2013-2015, he was a part time worker in position of research assistant at the Geomechanics Research Unit, Institute of Engineering, Suranaree University of Technology.

